DEVELOPING A CHEMOENZYMATIC LABELING TECHNIQUE

TO PROBE O-MANNOSE MODIFIED POLYPEPTIDES

by

ANURADHA R. KOPPIKAR

(Under the Direction of Lance Wells)

ABSTRACT

O-linked mannose has been implicated in cell-cell and cell-matrix adhesion. Defects in glycosyltransferases that add or extend O-linked mannose on glycoproteins generate neuron migration defects in congenital muscular dystrophies (CMD). The only well characterized O-mannose modified mammalian protein has been the peripheral membrane protein alpha-dystroglycan (α-DG). We propose that there must be other O-mannosylated proteins that modulate the CMD phenotype since O-mannosylation comprises a third of all O-linked glycans in the brain, and a brain α-DG knockout does not recapitulate all neuronal aspects of CMD. This research proposal aims to develop a chemoenzymatic labeling method to identify those proteins. Elucidating the functional role of O-mannose would contribute towards existing knowledge of how extracellular glycosylation participates in a broad range of human disorders and tissue functions while also paving the way for glycopeptide and enzyme based therapeutics.

KEYWORDS: O-Mannose, Neuron Migration, Chemoenzymatic Labeling

USING CHEMOENZYMATIC LABELING TO PROBE O-MANNOSE GLYCOSYLATION

By

ANURADHA R. KOPPIKAR

B.S., Georgia Institute of Technology, 2005

A Thesis Submitted to the Graduate Faculty of The University of Georgia in Partial Fulfillment of the Requirements for the Degree

MASTER OF SCIENCE

ATHENS, GA

2008

USING CHEMOENZYMATIC LABELING TO PROBE O-MANNOSE GLYCOSYLATION

by

ANURADHA R. KOPPIKAR

Major Professor: Lance Wells

Committee: Carl Bergmann

Michael Pierce

Michael Tiemeyer

Electronic Version Approved:

Maureen Grasso

Dean of the Graduate School

The University of Georgia

August 2008

To my teachers.

ACKNOWLEDGEMENTS

I thank my colleagues who shared the work on this project: Dr. Kazuhiro Aoki, Jae-Min Lim, Stephanie Hammond, Mindy Porterfield, and Karolyn Troupe. I thank all the Wells lab members, Tiemeyer lab members, and Pierce lab members who trained me in basic laboratory techniques during my tenure as a rotation student especially my supervisors in each lab starting with Dr. Kazuhiro Aoki, Dr. Gerardo Manilla-Alvarez, Enas El-Karim, and Jae-Min Lim. I thank my co-workers Peng Zhao, Meng Fang, Krithika Vaidyanathan, Edith Hayden, Sandii Brimble, and Chin Fen Teo for their valuable insights and suggestions. I thank our collaborators who supplied key reagents including Dr. David Live (UGA), Dr. Mian Liu (UGA), Dr. Huaiyu Hu (SUNY), Dr. Peng Zhang (SUNY), Dr. Carolyn Bertozzi (UC Berkeley), Dr. Linda Hsieh-Wilson (CalTech), and Dr. Pradman Qasba (NCI-Frederick). My parents have always supported my decisions, and to them I owe all my gratitude. To my friends who have shared many an hour discussing new research in science, I credit a growing love for the subject. Most of all, I thank my committee members who have been pivotal in guiding the course of this project and steering it in the right direction: My major professor Dr. Lance Wells, and Drs. Carl Bergmann, Michael Pierce, and Michael Tiemeyer.

TABLE OF CONTENTS

PAGE

LIST OF TABLES

PAGE

LIST OF FIGURES

PAGE

CHAPTER 1

INTRODUCTION

O-linked mannose was first characterized in *Saccharomyces cerevisiae* (1), and subsequent work has demonstrated its presence in metazoans (2-5). The glycosyltransferases that catalyze initial steps in this post-translational modification are evolutionarily conserved across species (6). In mammals, their loss of function results in cell adhesion and migration defects in congenital muscular dystrophies (CMD) (7). In this context, the most well characterized O-mannosylated protein has been alpha-dystroglycan (α-DG) (Figure 1) (4,8). However, the loss of function of α-DG does not sufficiently explain the repertoire of neurogenesis defects culminating in a cobblestone lissenchephaly phenotype in CMDs, especially since a third of O-glycans released from the brain are O-mannose initiated structures (9). We propose to address this disconnect by developing a chemoenzymatic labeling strategy (Figure 2) towards identifying other O-mannose modified proteins in the mammalian nervous system, and establishing a causal relationship between O-linked mannose and protein function.

O-linked mannose in mammalian nervous tissue. It is estimated that approximately a third of all O-linked glycans in the mammalian brain are O-mannose initiated structures (9). Traditionally, O-mannose has been linked to proteins in yeast and fungi where it has been implicated in protein secretion, cell wall integrity, and budding processes (10). In mammals, O-linked mannose was initially identified in bovine nerve alpha-dystroglycan (4) and in a rabbit brain protein reacting with the HNK-1 (LEU, CD57) monoclonal

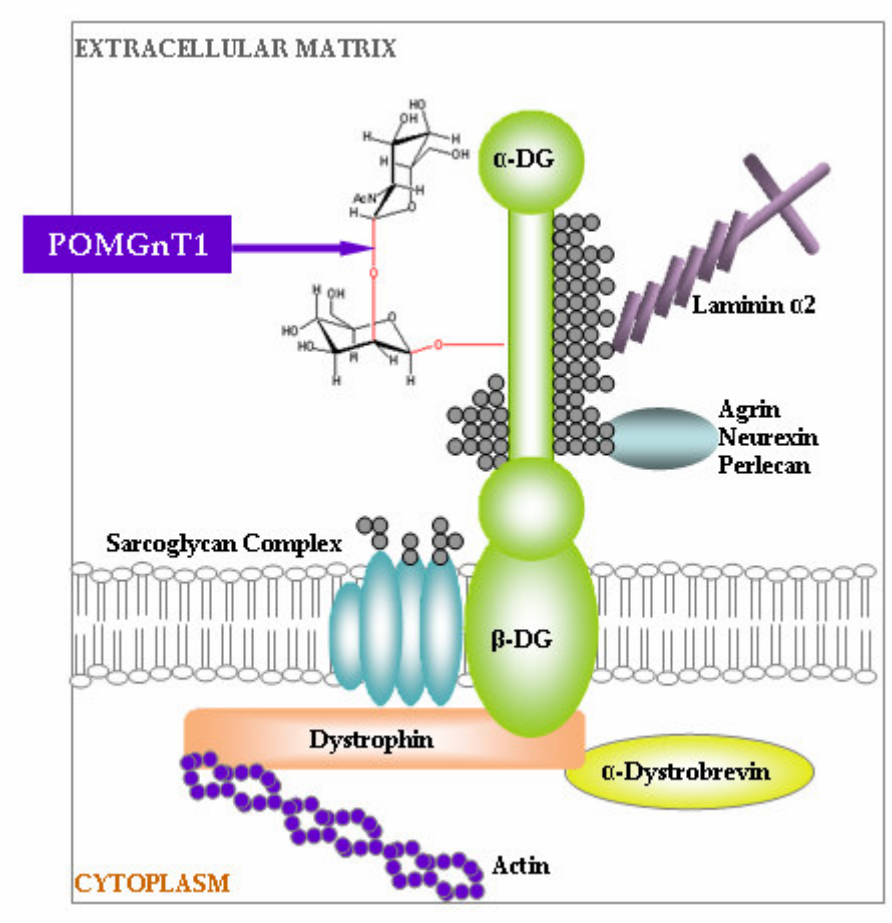

Figure 1. POMGnT1 adds a GlcNAc onto O-mannose moieties on alpha-dystroglycan. Positioned at the interface of the extracellular matrix and cytoskeletal elements, the α-subunit of dystroglycan (α-DG) and its binding partner laminin-2 interact via glycan structures. This is transduced to the cytoskeleton through a complex of proteins that include the β-subunit of dystroglycan, sarcoglycans, dystrobrevin, and dystrophin. Adapted from (11).

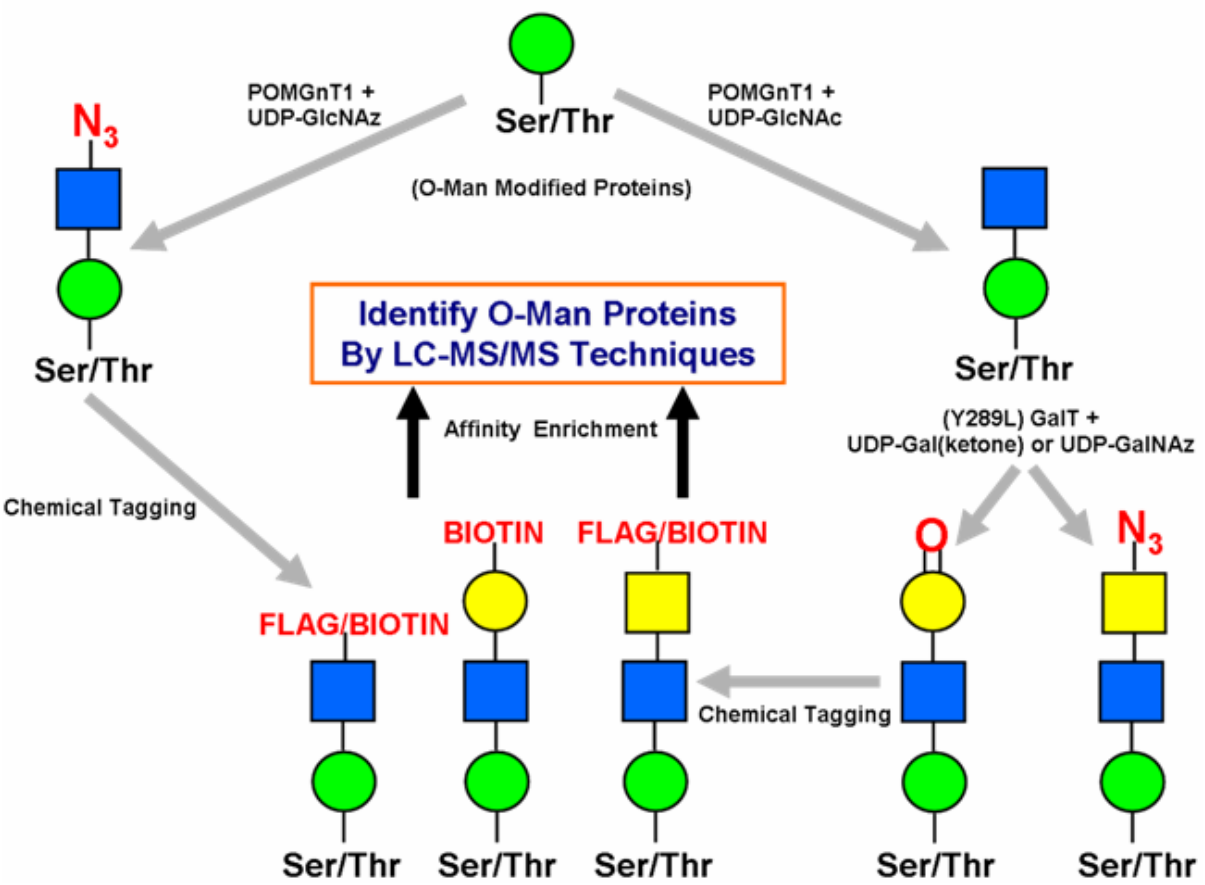

Figure 2. Experimental workflow for chemoenzymatic labeling strategies. Used with permission from Dr. Lance Wells (UGA).

antibody (5). Subsequent studies have identified additional O-linked mannose structures (4), and this work has been corroborated by studies conducted in our laboratory (Figure 3). Mammalian O-mannosylation involves a common core tetrasaccharide Siaα2-3Galβ1-4GlcNAcβ1-2ManαSer/Thr (12) that can also be observed as Galβ1-4GlcNAcβ1-2Manα1-3Ser/Thr, GlcNAcβ1-2ManαSer/Thr, GlcNAcβ1-2(GlcNAcβ1-6)ManαSer/Thr, or Siaα2-3Galβ1-4(Fucα1-3)GlcNAcβ1-2ManαSer/Thr structures (13). The presence of 3'-sulfoglucuronic acid, another acidic glycan in place of sialic acid on

A

ND = not detected		POMGnT1 -/-	POMGnT1 +/+
MW	Structure	% total	% total
534.6	GlcNAcMan	ND	7.91
	GalGalNAc	24.6	7.30
575.7	HexNAcGalNAc	0.9	0.4
738.9	GalGlcNAcMan	ND	1.5
896..0	SAGalGalNAc	28.3	16.8
913.1	Gal(Fuc)GlcNAcMan	ND	17.2
926.0	NeuGcGalGalNAc	2.6	2.3
937.1	SAHexNAcGalNAc	1.8	0.7
1100.3	SAGalGlcNAcMan	ND	6.1
1158.3	Gal(Fuc)HexNAc(Hex)GalNAc	0.1	0.1
1188.4	Hex2HexNAc(Hex)GalNAc	0.1	<0.1
1257.4	SAGa(SA)lGalNAc	35.8	33.5
1287.4	SA(NeuGc)GalGalNAc	2.3	1.9
1298.5	SAHexNAc(SA)GalNAc	1.8	1.6
1345.5	SAGalGlcNAc(GlcNAc)Man	ND	0.5
	SAHexHexNAc(Hex)GalNAc	0.6	0.5
1549.8	SAGalGlcNAc(GalGlcNAc)Man	ND	0.3
	Hex2HexNAc(SAHex)GalNAc	0.2	0.2
1618.8	SASAHex(SA)GalNAc	0.8	0.9
1706.9	SAHexHexNAc(SAHex)GalNAc	0.1	0.1
1911.2	SAGalGlcNAc(SAGalGlcNAc)Man	ND	0.2

B

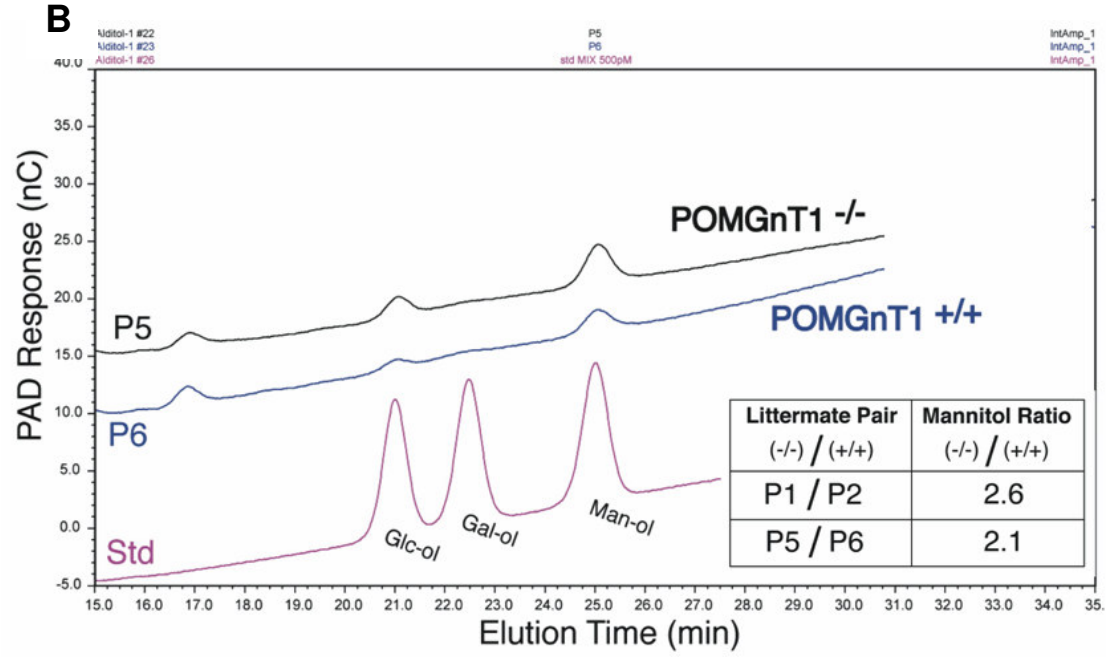

Figure 3. O-Glycans released from newborn mouse brain proteins. The **(A)** total MS profile (work performed by Jae-Min Lim, Dr. Kazuhiro Aoki, and Stephanie Hammond) and **(B)** monosaccharide chromatography trace of glycans from the POMGnT1

knockout mice display an absence of elongated O-Man initiated glycans, but an abundance of mannitol (work performed by Dr. Kazuhiro Aoki). Monosaccharides were released from protein, separated, and detected from POMGnT1 knockout (P1, P5) and wildtype mouse brains (P2, P6). Non-extended O-mannose structures are enriched ~2.4 fold in the POMGnT1 knockout mice. ND, Not determined.

Galβ1-4GlcNAcβ1-2Manαser/Thr results in an HNK-1 epitope that is expressed on molecules mediating both cell-cell and cell-matrix recognition and adhesion in the developing nervous system (5).

Loss-of-function of glycosyltransferases in the O-mannosylation pathway leads to CMDs (Table 1). The length of the O-mannose glycan directly affects the severity of the symptoms that include brain abnormalities and ocular defects (Table 2). Muscle-eye-brain disease (MEB) is a CMD resulting from the loss-of-function of the glycosyltransferase protein O-linked mannose beta1,2-N-acetylglucosaminyltransferase (POMGnT1) that transfers N-Acetylglucosamine (GlcNAc) from UDP-N-Acetylglucosamine (UDP-GlcNAc) in a β(1,2) linkage onto α(1,3) mannose on serine or threonine residues (7,13,14).

A MEB disease model organism would be ideal for identifying O-mannose substrates and elucidating glycan function owing to the absence of extended O-mannose structures, which in turn would allow for a pseudo bait and fish strategy using bioorthogonal chemical reporters (15) whereby O-mannosylated proteins could be tagged, isolated and identified. This strategy is described more in detail in the following sections.

TABLE 1. Muscular dystrophies associated with glycosylation of α-DG. The core tetrasaccharide Siaα3Galβ4GlcNAcβ2Manα-Ser/Thr is illustrated using the current symbol nomenclature adopted by the Consortium for Functional Glycomics. Adapted from (6,13).

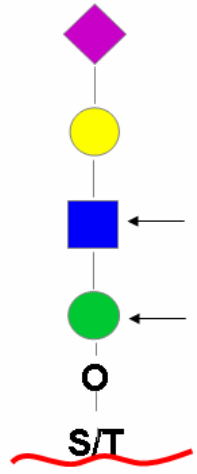

Gene	Biochemical Lesion	Disease	Biochemical Phenotype
LARGE	Putative glycosyltransferase, Golgi protein	MDC1D	Underglycosylated α-DG
Fukutin-Related Protein	Putative glycosyltransferase, Golgi protein	Limb-Girdle and MDC1C	Underglycosylated α-DG
Fukutin	Putative glycosyltransferase	Fukuyama-Type MDC	Underglycosylated α-DG
POMGnT1	GlcNAc β2 addition to O-Man	Muscle-Eye-Brain Disease	Underglycosylated α-DG, uncapped O-Man
POMT1/ POMT2	O-Man addition to Ser/Thr	Walker-Warburg Syndrome	Decreased protein O-mannosylation

MDC, Congenital Muscular Dystrophy; POMT1, Protein-O-Mannosyltransferase 1; POMGnT1, Protein O-linked Mannose β1,2-N-acetylglucosaminyltransferase 1

A mouse model of muscle-eye-brain disease was recently developed (18). The neurological phenotype observed in this POMGnT1 knockout mouse model demonstrates the function of O-linked mannose in the nervous system. Study of the cerebral cortex shows a disappearing pial basement membrane and glia limitans beginning at embryonic day 13.5, and culminating in a unique neuron overmigration phenotype marked by an abnormal distribution of Cajal-Retzius cells, changes in the radial glial morphology, disruption of the pia-arachnoid, ectopia of fibroblasts in the cortex, and reactive gliosis (18-20). Abnormal neuron migration phenotypes associated

TABLE 2. The length of the O-mannose glycan directly affects the severity of symptoms associated with congenital muscular dystrophy. Adapted from (14,16,17).

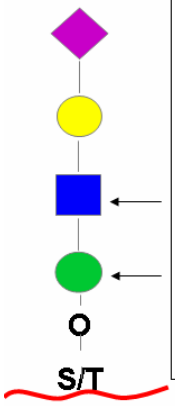

Disease	Phenotype	Age		
		Onset	Walk	Death
Muscle-Eye-Brain Disease	Cobblestone lissenchephaly, eye malformations, hydrocephalus, white matter changes present in infancy and early childhood.	Neonatal	Rarely	Toddlers
Walker-Warburg Syndrome	Cobblestone lissenchephaly, eye malformations, hydrochephalus, flat pons, cerebellar hypoplasia, white matter changes.	Neonatal	Never	Early infancy

with O-mannosylation are also evident in other organisms such as *Drosophila melanogaster* (21,22). Consequently, it can be postulated that O-linked mannose and its extended structures play an important role in neurogenesis.

Alpha-dystroglycan: A well-characterized O-mannosylated protein in mammals. The peripheral membrane protein, alpha-dystroglycan (α-DG) links the dystrophin-glycoprotein complex to the basal lamina (23), and is the most studied O-mannosylated protein in mammals. The transmembrane subunit of the DG complex, β-DG, forms a bridge between α-DG and the cytoskeleton. Nervous tissue DG is present in the hippocampus and cerebellar cortex, and in astrocytic basal lamina interfaces such as foot processes on cerebral blood vessels and foot processes at the pial surface of the brain and spinal cord (24). α-DG has been implicated in cell adhesion, migration, neurite extension, normal embryonic development beyond the egg cylinder stage, and assembly of ECM proteins (23).

Brain-selective deletion of dystroglycan in mice results in CMD-like brain malformations with phenotypes such as aberrant migration of granule cells due to impaired anchoring of radial glial processes, disarray of cerebral cortical layering, loss of interhemispheric fissure, and discontinuous pial basement membranes surrounding the cerebral cortex and cerebellum resulting in the fusion of cerebral hemispheres and cerebellar folia as observed in adult mice (25). The α-DG knockout brain also loses high-affinity binding to the extracellular matrix protein laminin as demonstrated by laminin binding and laminin overlay assays. This could be due to a defect in basement membrane formation, assembly, or stabilization, and is supported by phenotypes associated with mutations in α-DG ligands such as ECM β1-integrin, or the laminin γ1 chain (25).

Data derived from laminin binding, laminin overlay, surface plasmon resonance (SPR), and immunofluorescence experiments have determined that O-linked glycosylation of the core domain of α-DG mediates its binding to its ligands (23,26). Besides cell adhesion and migration, hypoglycosylation of α-DG and ligand binding has been linked to altered synaptic transmission, and blunted hippocampal long-term potentiation with electrophysiologic characterization. These phenotypes indicate a role for α-DG in learning and memory (25). This might be due to the fact that dystroglycan regulates neurotransmitter release as a synaptic structural element (27). O-linked glycosylation is also important for intracellular trafficking and targeting of proteins. Targeting of the secreted NMJ protein acetylcholinesterase is mediated by α-DG via the heparan sulfate proteoglycan, perlecan (28).

Given that the brain α-DG knockout does not recapitulate all aspects of CMD (Table 3), and that one third of brain O-glycans are O-mannose initiated structures, we hypothesize that there must be other O-mannosylated proteins in the mammalian brain.

TABLE 3. The α-DG knockout mouse model does not recapitulate all neuronal aspects of MEB (25).

Similarities
• Reduced laminin binding in the KO mouse brain is accompanied by disruptions of the glia limitans and neuronal migration errors, disarray of cerebral cortical layering, fusion of cerebral hemispheres and cerebellar folia, and aberrant migration of granule cells. • Immunofluorescence and ultrastructural analysis of both cerebral and cerebellar cortical surfaces reveals widespread discontinuities of the glia limitans accompanied by glial neuronal heterotopia within the leptomeninges. • Reduction in the high-affinity laminin binding of DG-null brain suggests that the mechanism underlying the disruptions is a loss of ability to organize the basal lamina of the glia limitans.
Differences
• Fusion of the cerebral interhemispheric fissure and adjacent cerebellar folia, multifocal disarray of neuronal layering in the cerebral cortex, malformations resembling polymicrogyria, and well-defined heterotopia within the superficial cortex is apparent in the DG-null mice, but does not occur in all CMDs. • Minor dispersion of neuronal cell bodies in the CA1 region and focal irregularities of the dentate granule cell layer are seen in the hippocampus of some DG-null mice, although major white-matter tracts are not remarkable. • The axon guidance defect not recapitulated. • GFAP-Cre/DG-null mice are fertile and have no gross neurological abnormalities. • All mice have well-formed corpus callosa, anterior cerebral arteries and lateral ventricles. This distinguishes the midline fusion in DG-null mice from holoprosencephaly. • Foliation progresses in normally in DG-null mice. However, there are residual nests of external granule cells in adult mice. • Baseline neurotransmission is unaffected in the DG-null mice. • Deficiency of dystroglycan does not affect presynaptic neurotransmitter release.

Based on the phenotype displayed by knockout animals of α-DG and POMGnT1, these proteins may include members of the heparan sulfate proteoglycan family (HSPGs) and chondroitin sulfate proteoglycan family (CSPGs) that have been implicated in axon guidance, pathfinding, and neuron migration (29). The research described herein purports to develop a chemoenzymatic labeling technique to directly isolate and identify O-mannosylated proteins based on well-established chemistries such as the Staudinger ligation and keto-aminooxy chemistry.

Bioorthogonal chemical reporter strategies to probe O-mannose modified polypeptides. Glycoproteins have been conventionally identified or isolated using an array of techniques such as lectins, antibodies, radioactive labeling, and liquid chromatography. However, these tools contain potential pitfalls within the context of identifying mammalian O-mannose modified polypeptides. Lectins require multiple binding sites for most ligands. Antibodies and antibody conjugates can be developed to recognize and adhere to specific ligands and possess high affinity to their antigens, although like radioactive labeling, they don't allow for direct identification of glycoproteins as compared to mass spectrometry. These techniques also have limited sensitivity. Liquid chromatography coupled with mass spectrometry is a robust tool. However, using liquid chromatography as a standalone tool makes it difficult to distinguish O-mannosylated peptides from glucolated, or galactosylated peptides. Mass spectrometry is often employed in high-throughput studies of post-translational modifications, and the following chemoenzymatic labeling strategies will take advantage of this instrument.

The past few years have seen a plethora of research directed towards the development and design of bioorthogonal chemical reporters in a number of biological applications. In general, this approach involves a two step labeling strategy, which in turn confers two degrees of specificity. In the first step, either native or recombinant glycosyltransferases transfer an unnatural synthetic monosaccharide onto the glycan of interest. These sugars contain a chemical handle such as a ketone, or an azide which can be chemoselectively ligated to reporter moieties such as FLAG or biotin (15). Studies comparing these synthetic monosaccharides to natural sugars have proven that both are recognized and transferred with a similar specificity by glycosyltransferases, and are stable. Some *in vitro* studies have also been conducted using recombinant glycosyltransferases with site mutations that allow recognition of the reporter sugars. This is the case with the mutant galactosyltransferase Y289L which was engineered by Dr. Pradman Qasba and colleagues. The mutation in this recombinant enzyme allows it to recognize and transfer either the natural substrate N-acetylgalactosamine (GalNAc), an unnatural galactose donor which harbors a ketone group at the C2 position, or an unnatural galactose donor which harbors an azide moiety (30,31).

The advantages of the bioorthogonal chemical reporter strategy are that it confers both enzymatic and chemical specificity, can be used both *in vitro* and *in vivo* depending on the chemical reporter in question, does not modify the native substrate conformation, forms a stable bond that can allows the substrate to be “fished” using affinity chromatography, and forms byproducts that are not reactive species. So far, this strategy has been used for studying sialic acid (Sia) (32,33), N-acetylglucosamine (GlcNAc) (34), and N-acetylgalactosamine (GalNAc) (35). Tagging the terminal O-

mannose residues with these functionalities will allow for a higher molecular weight species to be detected under neutral loss in collision-induced dissociation (CID) mass spectrometry. Following are two functional groups that have been tested for the purposes of this project.

a. Azides. Azides are useful as bioorthogonal reporter tags owing to several properties including a high intrinsic energy content and stability (15). Additionally, organic forms of this compound are not toxic, are resistant to oxidation, do not react with water, and are not present in nature. It is a mild electrophile that reacts with soft nucleophiles. Accordingly, it has been used for developing the Staudinger ligation with phosphines, and copper-catalyzed [3+2] azide-alkyne cycloaddition, or “click” chemistry (15).

The selectivity and speed of the Staudinger reaction (32) makes it useful for tagging complex biomolecules. In this reaction, the azide group suffers a nucleophilic attack from a triarylphosphine to form an aza-ylide intermediate. Subsequently, the intermediate traps a methoxycarbonyl group on an aryl ring of the phosphine to form an amide-linked phosphine oxide following hydrolysis. The reaction occurs at pH 7 at physiological temperatures with no side effects except phosphine oxidation by air or metabolic enzymes. Due to this reason, the Staudinger ligation has been used in a number of applications such as tagging glycans with azido sugars *in vivo* (36), enriching glycan-specific glycoproteins from cell extracts *in vitro* (34), creating small molecule arrays (37), and adding new functions to recombinant proteins (38).

The copper-catalyzed [3+2] azide-alkyne cycloaddition, or “click” chemistry is a modified form of the Huisgen 1, 3-dipolar cycloaddition (39). Morten Meldal and K. Barry Sharpless discovered that Cu(I) acts as a catalyst for cycloaddition between azides and

alkynes and accelerate the rate of the reaction (40,41). This reaction results in the formation of 1,4-disubstituted triazoles due to the property of azides as 1,3-dipoles that react with activated alkynes and other dipolarophiles. The advantage of this method is its specificity and that the rate of the reaction is 25 times more than the Staudinger ligation. “Click” chemistry has been used in studies with azide-labeled proteins from cell extracts (42), azide-labeled glycans (33), nucleic acids (43), and virus particles (44).

b. Ketones. Ketones are mild electrophiles which can serve as versatile chemical handles. They are neutral, and can be introduced easily into a number of substrates. However, these reactions can only occur at pH 5-6. Moreover, keto metabolites such as free sugars, pyruvate, oxaloacetate and cofactors such as pyridoxal phosphate are abundant in the intracellular environment. Consequently, ketones can be considered as “biorestricted” reporters, and are best used *in vitro* and in the absence of carbonyl electrophiles (15). Linda Hsieh-Wilson and colleagues have spearheaded an approach using a ketone reaction with an aminooxybiotin nucleophile to enrich and identify O-linked GlcNAc modified proteins from cell extracts (45). As mentioned at the beginning of this section, this strategy utilizes a mutant galactosyltransferase Y289L which can recognize and transfer the unnatural ketone sugar substrate. Other research has been devoted towards drug synthesis (46) and the development of drug delivery systems (47).

The Staudinger ligation, “click” chemistry, and keto-aminooxychemistry together offer a comprehensive approach towards labeling O-mannose modified polypeptides from mammalian brain extracts. Using three approaches will reduce the false error rate during mass spectrometric analysis of glycoproteins enriched from cellular extracts.

However, neither of these approaches has been engineered towards tagging and identifying O-mannosyl substrates. Moreover, they rely on the availability of the enzymes POMGnT1 and Y289L GalT, an unnatural sugar donor, a substrate possessing terminal O-linked mannose moieties, and a chemical tag. Chapter 2 discusses method development for these approaches, while Chapter 3 delves into potential experiments that can be undertaken towards the overall goal of elucidating the O-mannose structure-function relationship in the mammalian nervous system.

CHAPTER 2

RESULTS AND DISCUSSION

This project was devoted towards developing a chemoenzymatic labeling technique for isolating O-mannosylated proteins via affinity chromatography and identifying them via HPLC and mass spectrometry. A synthetic α-DG derived O-mannose peptide, Ac-VEPT(Man)AV-NH_2 (a gift from Dr. David Live, UGA) was used as a substrate in order to demonstrate the reliability of this technique. Future studies will utilize brain extracts from a POMGnT1 knockout mouse (a gift from Dr. Hyaiyu Hu). The chemoenzymatic labeling techniques rely on glycosyltransferase specificity towards unnatural sugar substrates that can be eventually tagged with chemoselective reporters such as FLAG and biotin. Affinity purification of these reporter tags will be followed by LC-MS/MS and other mass spectrometry based studies.

The POMGnT1 knockout mouse has terminal O-mannose residues which do not get extended by other glycosyltransferases.

(a) Glycan characterization of wildtype and POMGnT1 knockout mouse brains. Work performed by Dr. Kazuhiro Aoki, Jae-Min Lim, and Stephanie Hammond. Evaluating the O-glycan profile was critical before proceeding to chemoenzymatic labeling because O-mannose initiated structures are known to be extended, with the predominant structure being a core unbranched tetrasaccharide: Sia(α2-3)Gal(β1-4)GlcNAc(β1-2)Man(α1-3)Ser/Thr.

METHOD: Total brain proteins from a mouse model of Muscle-Eye-Brain disease (work done in collaboration with Dr. Haiyu Hu, SUNY) and their wild-type littermates were subjected to organic extraction, delipidated, and intact O-linked glycans were released by reductive β-elimination (48). Mouse brains were weighed, and ground to a fine powder in liquid nitrogen using a mortar-pestle. The powder was delipidated using a 4:8:3 ratio of chloroform:methanol:water using a dounce homogenizer on ice. The contents were centrifuged at 3500 rpm at 4˚C for 15 minutes following a six hour incubation on a shaker at room temperature. Water and acetone were added in a 1:4 ratio to the samples, vortexed, incubated on ice for 15 minutes, and centrifuged at 3500 rpm at 4˚C for 15 minutes. This was repeated for a total of three cycles. The resulting supernatant at the end of each centrifuge cycle was collected as lipid and dried in a speedvac, while the final pellet was dried under nitrogen gas at 45˚C. The dried protein powder was stored at -20˚C.

To release glycans, an aliquot of the powder was incubated in sodium hydroxide and sodium borohydride at 45˚C for 16 hours. At the end of the incubation, the samples were neutralized using 10% acetic acid and applied to an AG50W-X8 cation exchange column (Bio-Rad). The eluate was desalted using a C18 reverse phase column, and concentrated to dryness using a speedvac. Part of the sample was permethylated for glycan sequence analysis and quantification via LC-MS^n on a linear ion trap (ThermoFisher LTQ), while the rest was hydrolyzed with 2M trifluoroacetic acid, injected into a high pH anion-exchange chromatographic (HPAEC) CarboPA1 column (Dionex), and quantified with a pulsed amperometric detector (Dionex). The procedure for permethylation requires the addition of a freshly prepared suspension of sodium

hydroxide in DMSO i.e. base to the sample followed by the addition of iodomethane. After purging with nitrogen gas, the sample was cleaned up via aqueous–organic extraction, and concentrated to dryness using a speedvac before injection into the mass spectrometer. Data was analyzed via Total Ion Mapping (TIM scan) using XCalibur software (version 2.0) as demonstrated previously (49).

RESULTS: The results show that the O-mannose moieties in knockout mouse brains did not have extended O-mannose linked structures as confirmed via MS/MS (Figure 3A). This demonstrates the requirement for POMGnT1 during extension. Moreover, the knockout mouse brains had elevated levels of mannitol as compared to their wild-type littermates (Figure 3B), which might occur because mannose moieties do not get extended in the POMGnT1 knockout mouse. As shown previously by using other techniques (9), we can demonstrate via MS/MS that a third of the observed O-linked glycans released from wildtype brain proteins are O-Man initiated (Figure 3A). The glycan profile also presents m/z data for setting up a neutral loss table necessary for tandem MS-based peptide sequencing. This sets the stage for the aforementioned pseudo bait-fish chemoenzymatic labeling techniques using POMGnT1.

OPTIMIZATION: The experimental conditions for reductive β-elimination were modified in order to reduce peeling reactions i.e. the formation of truncated glycans and degradation of certain peptide sequences which can result from high base concentration, high temperature, and longer incubation times.

(b) Western blots of chemoenzymatically labeled POMGnT1 knockout mouse brain extracts using “click” chemistry.

METHOD: Protein powder was made using brains from the POMGnT1 knockout mouse and the wildtype littermates as described in (a). The samples were chemoenzymatically labeled, affinity purified and detected on western blot as described below. Recombinant POMGnT1 enzyme was expressed using the vector pSecTag2B (collaboration with Dr. Huaiyu Hu, SUNY) containing the catalytic segment of POMGnT1 (Figure 4A). The vector was stably transfected into HEK-293T cells using Lipofectamine 2000 (Invitrogen) (work performed by Dr. Gerardo Alvarez-Manilla, Karolyn Troupe and Nicole Warren), and the cells were maintained in DMEM with high glucose and L-glutamine under 10% FBS, penicillin, streptomycin, and zeocin for three days. The 47-kDa recombinant enzyme was secreted into the cell media. Consequently, the cell media was collected and an EDTA-free protease inhibitor cocktail (Sigma) was added. This was buffer exchanged and concentrated using Centriprep YM-10 columns (Millipore), and the concentrate was applied to a Ni-NTA affinity resin (Qiagen). The wash buffer consisted of 25mM Tris buffer pH 7.5, 250mM NaCl, and 5mM imidazole pH 8.0. The fraction containing the most POMGnT1 enzyme activity was eluted using 25mM Tris buffer pH 7.5, 100mM NaCl, and 300mM imidazole pH 8.0. The eluate was subsequently desalted using a Sephadex-G25 column (GE Healthcare) (Figure 4B), and stored at 4˚C in 700µg/mL BSA, 10mM MES, 100mM sodium chloride, and 2mM manganese chloride. Enzyme activity was confirmed via radioactivity using tritiated UDP-GlcNAc and a standard substrate benzyl mannose (Figure 4C-D) (50). The POMGnT1 enzymatic assay was run for 6 hours at 37˚C, and consisted of

A


TM
Stem
Catalytic
N
C
1
38
59
301
660

B

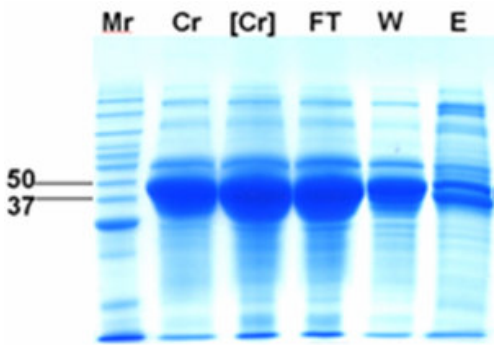
Mr
Cr
[Cr]
FT
W
E
50
37

C

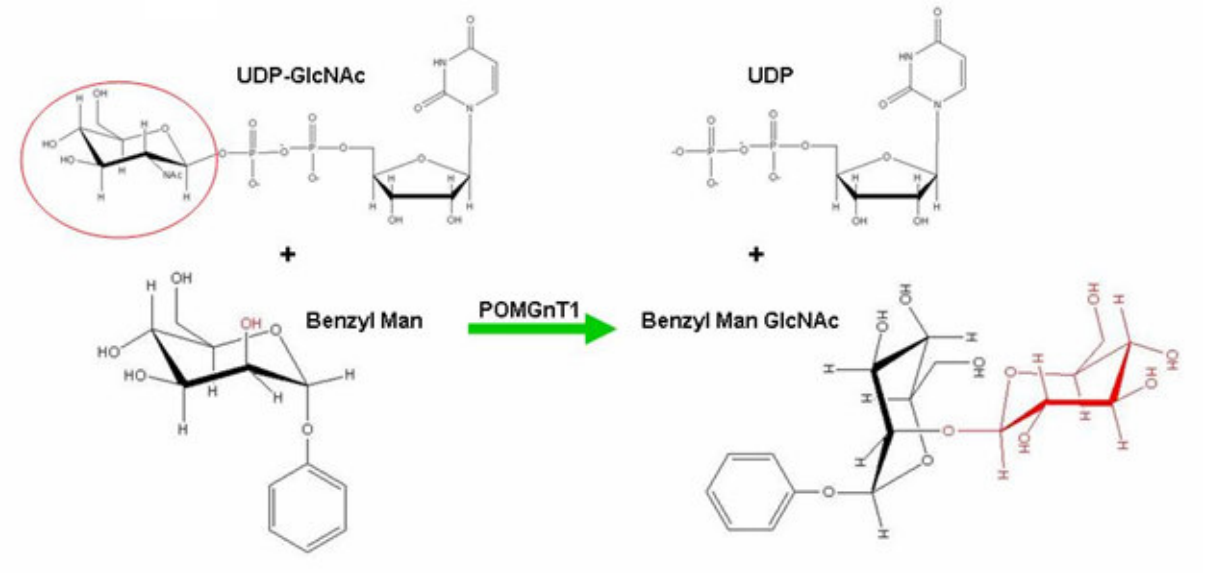
UDP-GlcNAc
UDP
+
+
Benzyl Man
POMGnT1
Benzyl Man GlcNAc

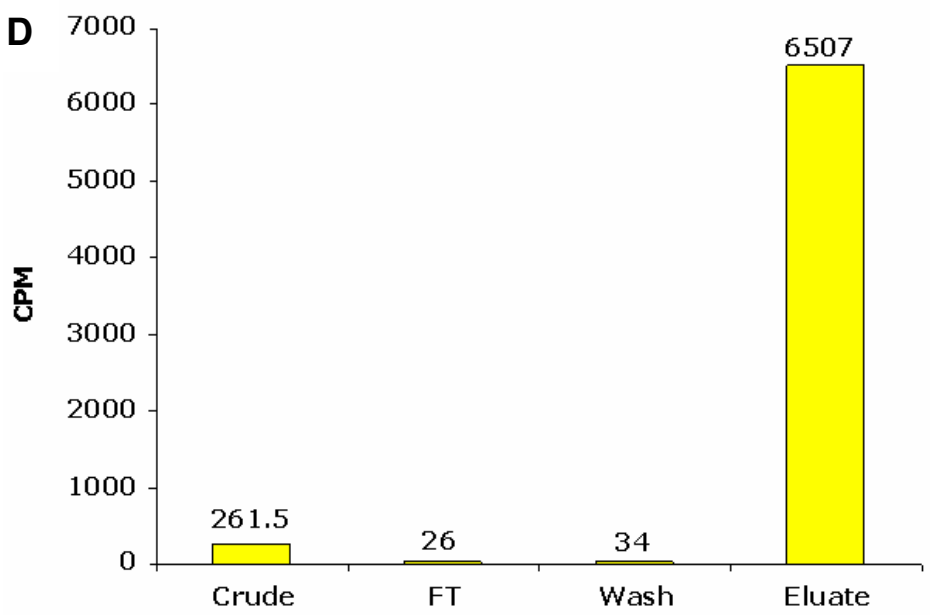

Figure 4. Enrichment of recombinant POMGnT1. **(A)** A vector containing the catalytic segment of the 660 amino acid POMGnT1 was transfected into HEK-293T cells (work performed by Gerardo Alvarez-Manilla, Karolyn Troupe, and Nichole Warren), and **(B)** the 47kDa secreted enzyme was enriched using nickel affinity. **(C)** A radioactive assay using tritiated UDP-GlcNAc and benzyl mannose shows **(D)** a higher activity against the nickel column eluate as compared to the other fractions. TM, Transmembrane; Mr, Marker; Cr, Crude; [Cr], Crude concentrate; FT, Flowthrough; W, Wash; E, Eluate.

10mM UDP-GlcNAc, 20mM benzyl mannose, 1 x 10^5 cpm ^{3}[H]-UDP-GlcNAc, 12.5mM $MnCl_2$, 50mM MES pH 6.5, and a unit of alkaline phosphatase per 20µL reaction volume. The nickel column eluate carrying POMGnT1 enzyme activity comprised a fifth of the total reaction volume. POMGnT1 activity was further confirmed via POMGnT1 labeling of a synthetic α-DG derived O-mannose modified peptide (a gift from Dr. David

Live, UGA) using the similar reaction conditions albeit in the absence of 1 x 10^5 cpm ^{3}[H]-UDP-GlcNAc. The assay was run for 12 hours at 37˚C. Product formation was monitored and separated on a C18 reverse phase HPLC column (Agilent 1100) (Figure 5A) followed by direct infusion of the product peak into a linear ion trap (LTQ, ThermoFinnigan) (Figure 5B).

POMGnT1 knockout and wildtype adult mouse brains were subjected to dounce homogenization and delipidation in order to make protein powder as described in (a). Brain powder was prepared for the POMGnT1 reaction by adding in 0.1% SDS and 0.9% NP-40, heating at 90˚C for 10 minutes, vortexing, sonicating, and cooling on ice for 3 minutes. The solubilized sample was subjected to the POMGnT1 reaction in 10mM UDP-GlcNAz (Invitrogen), 12.5mM $MnCl_2$, 50mM MES pH 6.5, and a unit of alkaline phosphatase per 20µL reaction volume. The POMGnT1 enzyme comprised a fifth of the total reaction volume. The samples were incubated at 37˚C for a total of 48 hours, with a fresh aliquot of POMGnT1 enzyme being added every 12 hours. A commercially available Click-iT™ Biotin Protein Analysis Detection Kit (Invitrogen) was used for labeling azido groups via “click” chemistry, which involves 1,3-dipolar cycloaddition between the azide and a biotin modified alkyne probe. The GlcNAz-labeled samples were boiled in SDS sample buffer, and separated on a 10% Tris-HCl polyacrylamide gel (BioRad) before transferring to a PVDF membrane. The membrane was blocked overnight at 4˚C in 3% non-fat milk (w/v) in 0.1%TBSt, and incubated in streptavidin horseradish peroxidase conjugate (GE Amersham) for 1h at room temperature (1:10000). Washed blots were developed in SuperSignal West Pico chemiluminescent substrate (51) exposed using CL-X Posure film (Thermo Scientific).

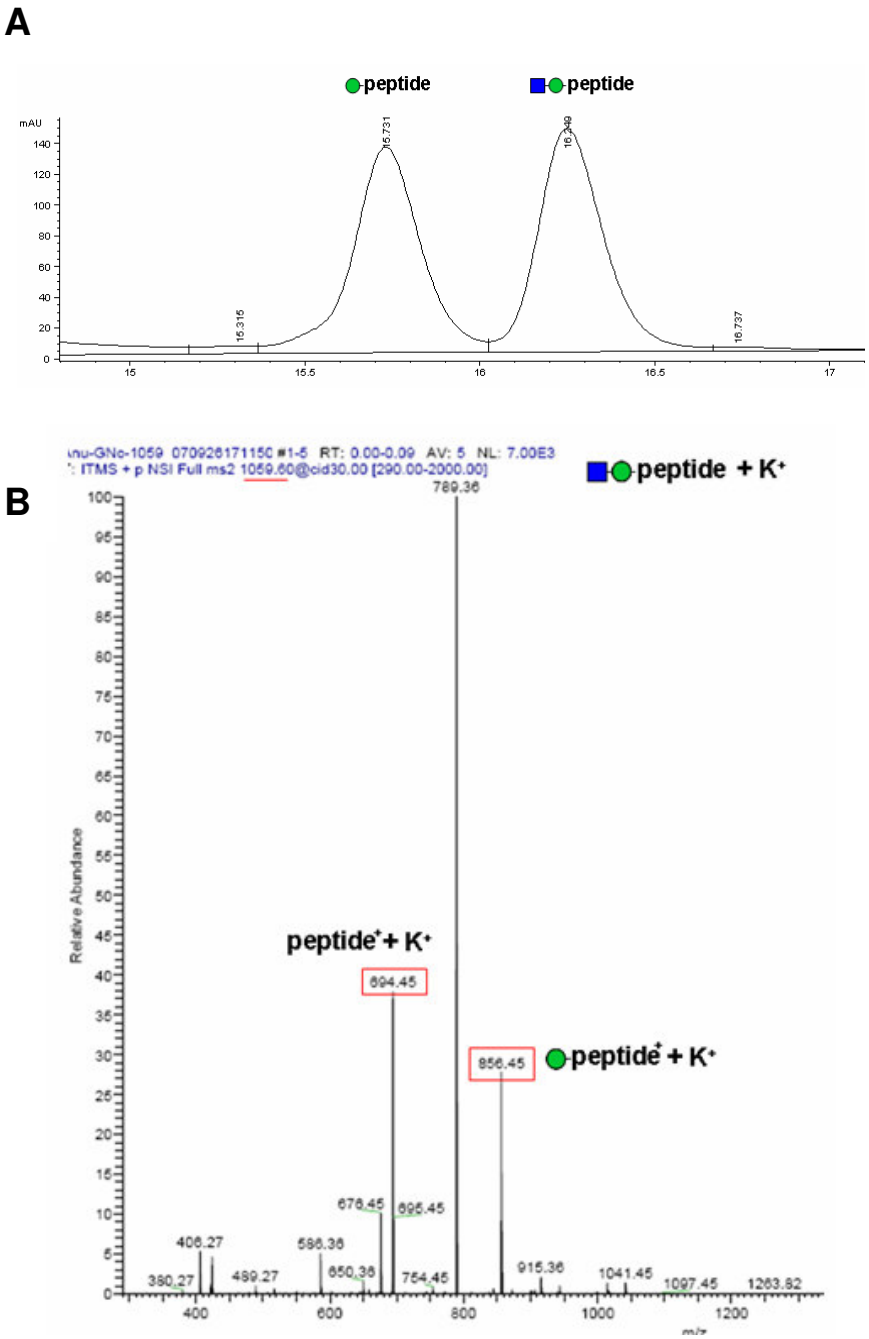

Figure 5. Evidence for the formation of the GlcNAc product. **(A)** HPLC trace monitoring the reaction 24h after the addition of UDP-GlcNAc and POMGnT1. **(B)** MS/MS fragmentation of 1059.60, the GlcNAc product formed in **(A)**. Peptide sequence, Ac-VEPT(Man)AV-NH_2

RESULTS: Nickel column purification of the HEK-293T cell media successfully enriched for a fraction containing POMGnT1 activity as demonstrated by the bands on the coomassie stained gel (Figure 4B), the higher radioactivity in the eluate fraction (Figure 4D), and the formation of the GlcNAc-Man-peptide as demonstrated by the HPLC data (Figure 5A) and fragmentation of the product peak by mass spectrometry (Figure 5B). Bovine serum albumin was added to the desalted POMGnT1 activity containing fraction so as to diminish the activity of matrix metalloproteinases which are possibly purified along with the recombinant POMGnT1 enzyme in the nickel column purification step (in correspondence, Dr. M. Pierce). The presence of multiple bands in the western blot for POMGnT1 knockout brain powder labeled with UDP-GlcNAz using POMGnT1 enzyme (Figure 6C) as compared to the control lanes containing the POMGnT1 enzyme reaction with UDP-GlcNAz only (Figure 6A), or the POMGnT1 enzyme reaction with UDP-GlcNAc and knockout mouse brain powder (Figure 6B) show that there are potentially other O-mannosylated proteins in the POMGnT1 knockout brain. Some background labeling was observed in the absence of the brain powder (Figure 6A), and it is postulated that the recombinant POMGnT1 enzyme itself might be an O-mannosylated protein. An alternative hypothesis is that the enzyme transfers GlcNAz onto O-mannosylated proteins pulled down in the nickel column eluate containing POMGnT1 enzyme activity.

OPTIMIZATION: Kinetic experiments using tritiated UDP-GlcNAc and benzyl mannose show that GlcNAc-benzyl mannose product formation reaches equilibrium in approximately 4 hours (data not shown). All brain powder labeling experiments were

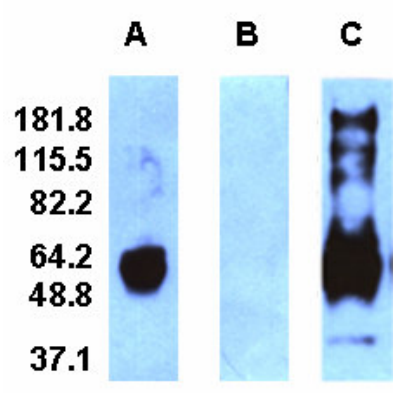

Figure 6. Evidence for multiple O-mannosylated proteins in the brain. Samples were chemoenzymatically labeled, biotinylated using “click” chemistry (Invitrogen), and western blotted. Control lanes for **(A)** POMGnT1 enzyme and UDP-GlcNAz, or **(B)** POMGnT1 enzyme, UDP-GlcNAc, and POMGnT1 knockout mouse extract show fewer bands compared to **(C)** the sample containing the POMGnT1 knockout mouse extract labeled using recombinant POMGnT1 enzyme and UDP-GlcNAz.

carried out for 12 hours before replenishing the enzyme. This reaction time could be reduced by first calculating the amount of POMGnT1 activity required in order to drive the man-peptide reaction to completion, and then determining the time that it takes for the enzyme to lose activity. The first can be tested by keeping the substrate concentration constant, and varying the amount of enzyme added. The reaction can either be tested via radioactivity, or it can be monitored via HPLC and confirmed via MS/MS. The time taken by POMGnT1 to lose activity can be tested by setting up a radioactive assay, and varying the time while keeping the amount of enzyme and substrate constant. Loss of POMGnT1 activity will be seen by a reduction in radiation counts. The results of these two experiments will not only reduce the time taken for the main experiment, but it will also allow for a reduction in the formation of degradation

products that might result due to a longer incubation time. It is not clear as to whether POMGnT1 labels itself with GlcNAz, or whether it labels other proteins that are in the nickel column eluate (Figure 6A). To bypass detecting POMGnT1 in future experiments using either western blots or mass spectrometry, we propose tagging the recombinant POMGnT1 to beads that can be affinity- or magnetically captured and removed after the reaction proceeds to completion.

Chemoenzymatic labeling of synthetic α-DG derived O-Mannose modified peptide using Staudinger ligation and keto-aminooxy chemistry. We have employed a bioorthogonal chemical reporter strategy that utilizes two different chemistries: Staudinger ligation, and keto-aminooxy chemistry. As described in Chapter 1, both are established methods for identifying certain O-linked sugars (31,34). However, neither of these has been used towards identifying O-linked mannose substrates. In the context of this project, they rely on the availability of the enzymes POMGnT1 and Y289L GalT, an unnatural sugar donor, a substrate possessing terminal O-linked mannose moieties, and a chemical tag. While some of these components were generated in-house, the rest are either commercially available, or have been procured from another laboratory. A synthetic alpha-dystroglycan derived O-Mannose modified peptide (in collaboration with Dr. David Live, UGA) was used during the method development of chemoenzymatic labeling studies in order to verify the reliability of the technique. This peptide sequence was discovered during experiments site-mapping O-mannosylation on α-DG in rabbit skeletal muscle (data not shown), and thus might be a putative sequence for POMGnT1 action. As described in the previous section, the viability of this peptide sequence was confirmed in a POMGnT1 reaction using UDP-GlcNAc (Figures 5A and 5B).

METHOD: The POMGnT1 reaction was carried out under similar reaction conditions as described in the previous sections using a 0.2mM substrate O-mannose peptide, donor 10mM UDP-GlcNAz (Invitrogen), and buffer sodium phosphate pH 7.5 instead of MES pH 6.5. A parallel reaction was carried out with donor 10mM UDP-GlcNAc (Sigma) under the same reaction conditions as described previously for use towards the two-step enzymatic reaction using a mutant Y289L GalT (a gift from Dr. Pradman Qasba) in the second step. The two-step ketone reaction was carried out using the GlcNAc-Man-peptide as a substrate and 25mM MOPS pH 4.5, 5mM $MnCl_2$, 1mM UDP-Gal-ketone (a gift from Dr. Linda Hseih-Wilson), 100ng/μL Y289L GalT, and a unit of alkaline phosphatase per 20μL reaction volume (52). The two-step azido reaction was carried out on the GlcNAc-Man-peptide using a commercially available O-GlcNAc labeling kit (Invitrogen). All products and intermediates were separated and monitored using HPLC (Agilent 1100) on a C18 reverse phase column. LC buffer A consisted of 0.1% formic acid and buffer B consisted of 0.1% formic acid, 80% acetonitrile. The gradient consisted of 0-3 min, 2% B; 3-6 min, 2-15% B; 6-15min, 15-16% B; 15-21min, 16-17%B; 21-30min, 17-100%B; 30-40min, 100%B. All peaks were confirmed using mass spectrometric analysis via nanospray into a linear ion trap (ThermoFinnigan LTQ). The samples were directly infused into the LTQ at a flow rate of 0.4 ul/min in 50% buffer A/50% buffer B.

The Gal(keto) components were labeled with aminooxybiotin (Dojindo) as described in (31). The azide labeled components were tagged with either FLAG-phosphine (Sigma) as described in (34), or with a commercially available O-GlcNAc detection kit that uses a biotinylated alkyne (Invitrogen). FLAG tagged components

were affinity purified using anti-FLAG M2 agarose resin (Sigma), while biotinylated components were affinity purified using monomeric avidin resin (51) as described by the manufacturers. The products were desalted using a C18 reverse phase spin column, and analyzed using a linear ion trap (ThermoFinnigan LTQ). The samples were directly infused into the LTQ at a flow rate of 0.4 ul/min in 50% buffer A/50% buffer B.

RESULTS: The synthetic O-mannose peptide was modified using one of two azido sugars: UDP-GlcNAz (Figure 7), and UDP-GalNAz (Figure 8). Recombinant POMGnT1 can directly/specifically transfer GlcNAz onto O-mannose sites, and this offers the distinct advantage of a lower false error rate during protein identification via mass spectrometry. Moreover, GlcNAz might be a preferred donor for POMGnT1 (Figure 7A) as compared to GlcNAc. The GlcNAz reaction products could be separated by HPLC only when the buffer MES pH 6.5 was substituted with sodium phosphate pH 7.5 (Figure 7C). MES might interfere with the azide reaction specifically with the man-peptide, since the western blots using POMGnT1 and UDP-GlcNAz to label mouse brain proteins (Figure 6) demonstrate that POMGnT1 can transfer GlcNAz under MES buffer conditions. The mass spectrum for the GlcNAz-Man-peptide product shows low signal intensity, and this might occur due to errors during fragment ion acquisition.

The second approach involves two step enzymatic labeling. Recombinant POMGnT1 transferred GlcNAc onto the Man-peptide, and this product was subjected to mutant Y289L GalT reaction to transfer GalNAz onto the terminal GlcNAc moiety. The azido groups can react either with a FLAG-phosphine via Staudinger ligation, or with a biotin-alkyne via “click” chemistry for subsequent affinity purification. The GalNAz

A

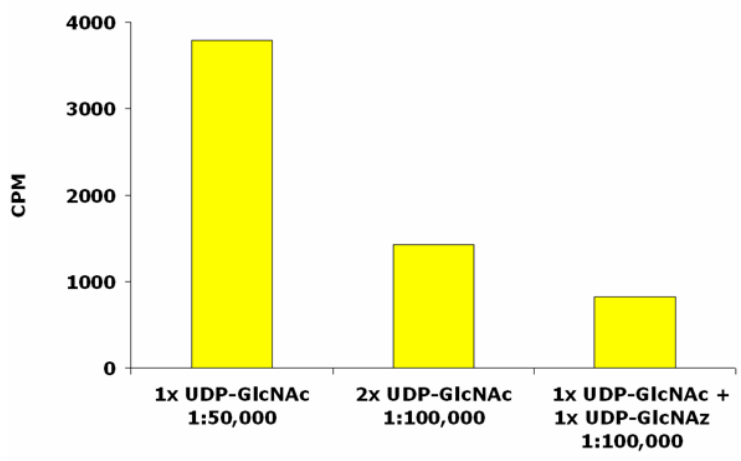
4000
3000
2000
1000
0
CPM
1x UDP-GlcNAc
1:50,000
2x UDP-GlcNAc
1:100,000
1x UDP-GlcNAc +
1x UDP-GlcNAz
1:100,000

B

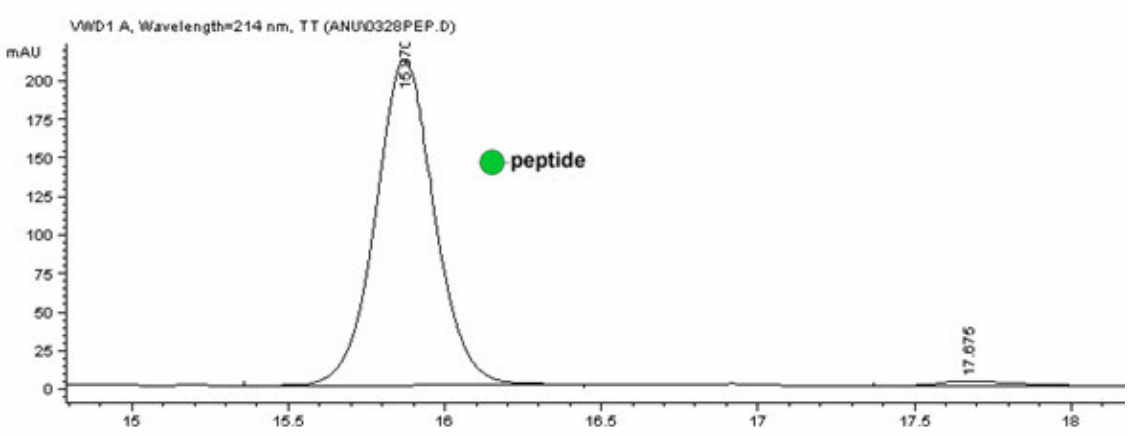
VWD1 A, Wavelength=214 nm, TT (ANU0328PEP.D)
mAU
peptide
17.676
15
15.5
16
16.5
17
17.5
18

C

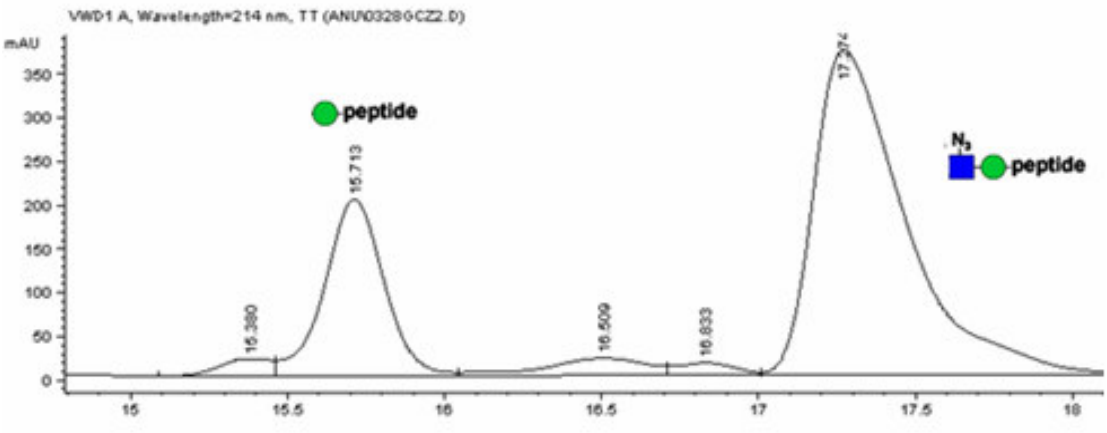
VWD1 A, Wavelength=214 nm, TT (ANU0328CZ2.D)
mAU
peptide
15.713
15.380
16.509
16.833
peptide
15
15.5
16
16.5
17
17.5
18

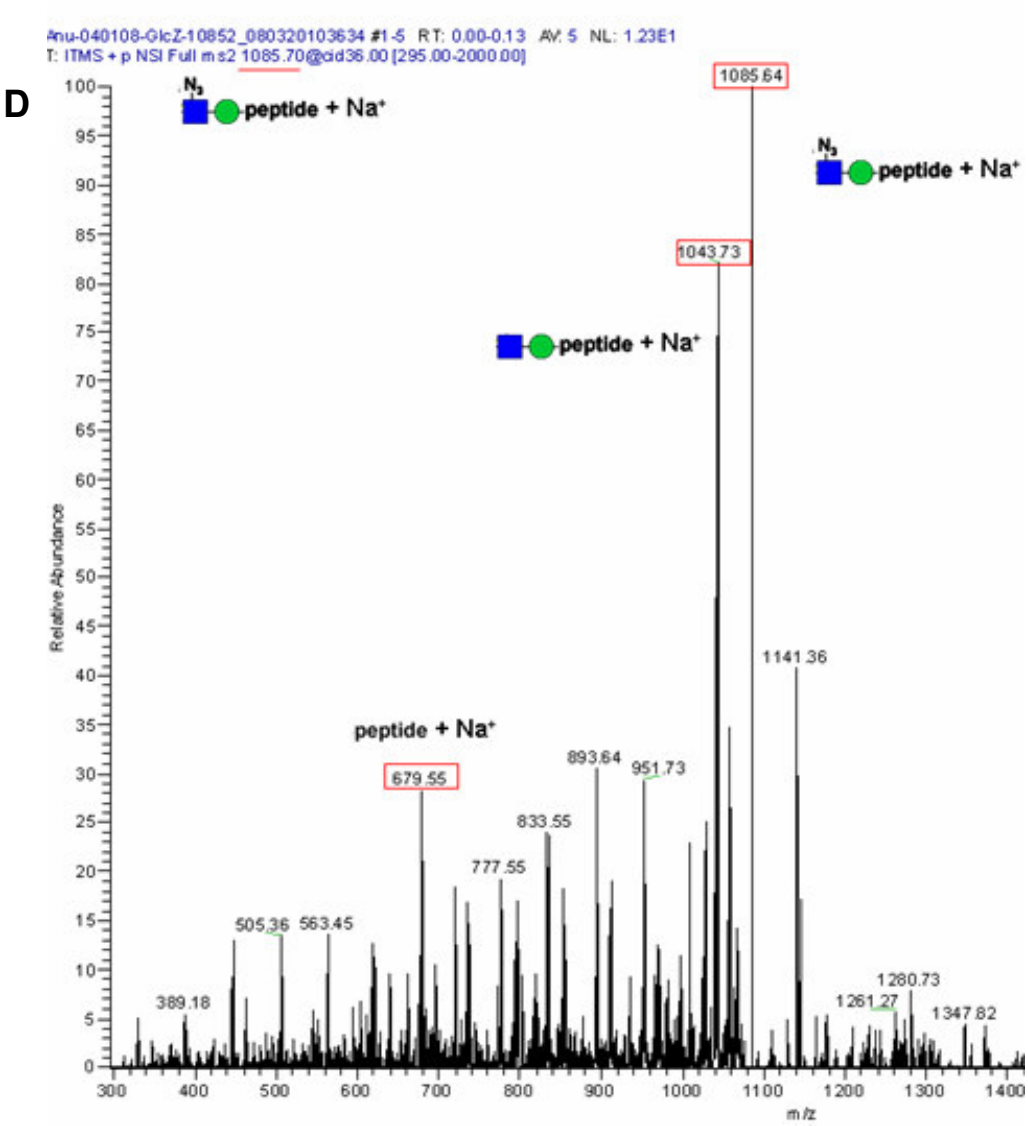

Figure 7. Evidence for the formation of the GlcNAz product. **(A)** Radioactivity demonstrates that UDP-GlcNAz is either a preferred donor, or a competitive inhibitor for POMGnT1 in an assay with benzyl mannose. Radioactive counts are reduced in half upon doubling the amount of cold UDP-GlcNAc, and a third upon adding equal amounts of cold UDP-GlcNAc and UDP-GlcNAz. HPLC traces monitoring the reaction at **(B)** time 0, **(C)** 24h after the addition of UDP-GlcNAz and POMGnT1. **(D)** MS/MS fragmentation of 1085.70, the GlcNAz product formed in **(C)**. Peptide sequence, Ac-VEPT(Man)AV-NH_2

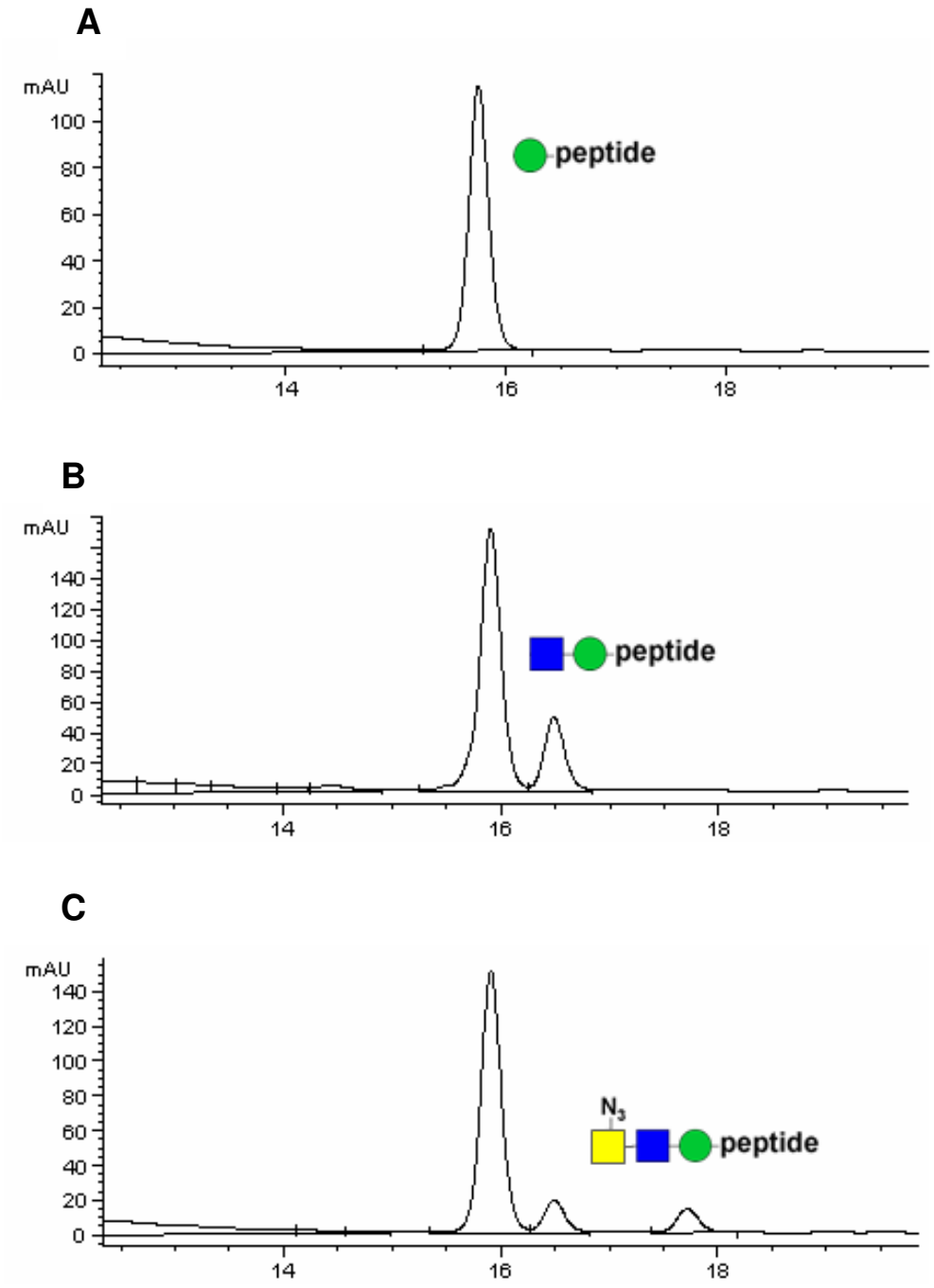
A
mAU
100
80
60
40
20
0
peptide
14
16
18
B
mAU
140
120
100
80
60
40
20
0
peptide
14
16
18
C
mAU
140
120
100
80
60
40
20
0
N3
peptide
14
16
18

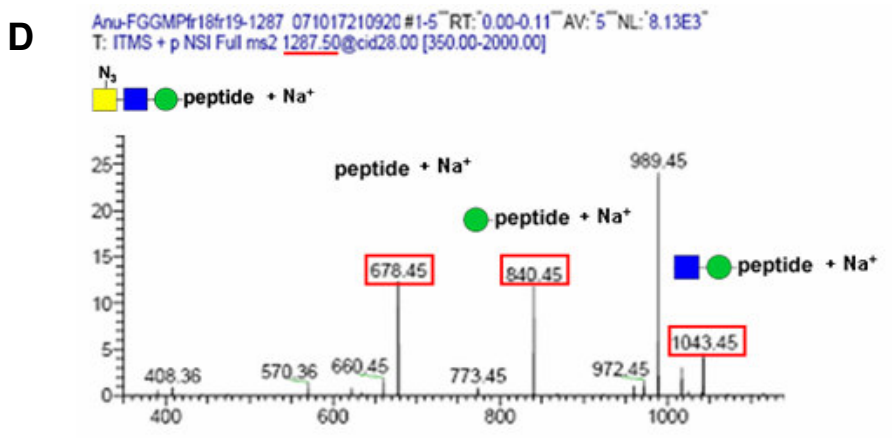

Figure 8. Evidence for the formation of the GalNAz product. HPLC traces monitoring the reaction at **(A)** time 0, **(B)** 24h after the addition of UDP-GlcNAc and POMGnT1, **(C)** 12h after the addition of GalNAz and Y289L GalT. **(D)** MS/MS fragmentation of 1287.50, the GalNAz product formed in **(C)**. Peptide sequence, Ac-VEPT(Man)AV-NH_2

product was created successfully (Figure 8). A contaminant appears in the affinity purified eluate of the FLAG-tagged product (data not shown). This might occur due to an error in the experimental technique, since this contaminant does not occur in the control experiment using only the anti-FLAG M2 agarose resin as a blank (data not shown).

The keto-aminooxy strategy also involves a two step enzymatic approach. Recombinant POMGnT1 transferred GlcNAc onto the Man-peptide, and this product was subjected to a mutant Y289L reaction involving the transfer of a keto-modifed sugar onto the terminal GlcNAc substrate and subsequent ligation with a chemoselective biotin-aminooxy tag (Figure 9). Unlike the contaminant occurring in the experiment using anti-FLAG M2 agarose resin, the biotin tagged Gal(keto)-GlcNAc-Man-peptide

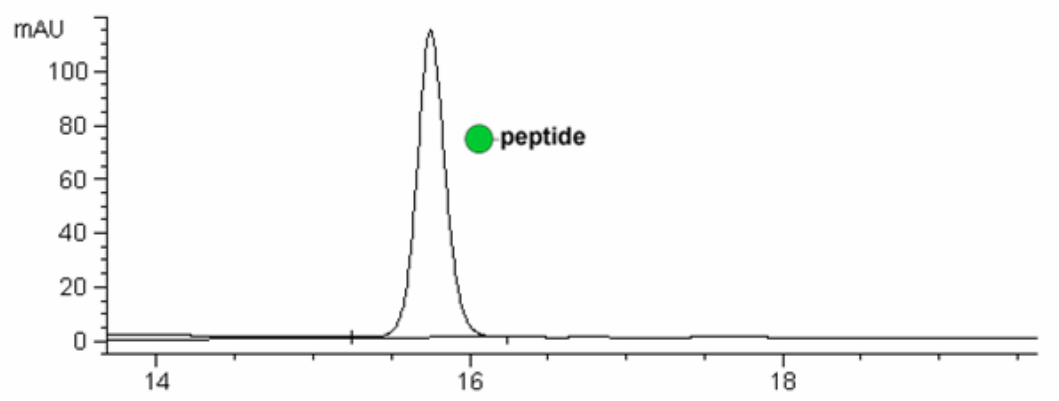
mAU
100
80
60
40
20
0
14
16
18
peptide

B

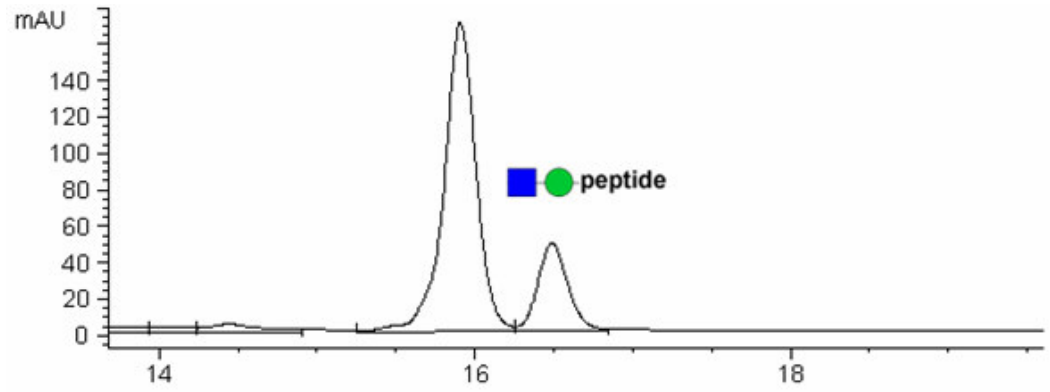
mAU
140
120
100
80
60
40
20
0
14
16
18
peptide

C

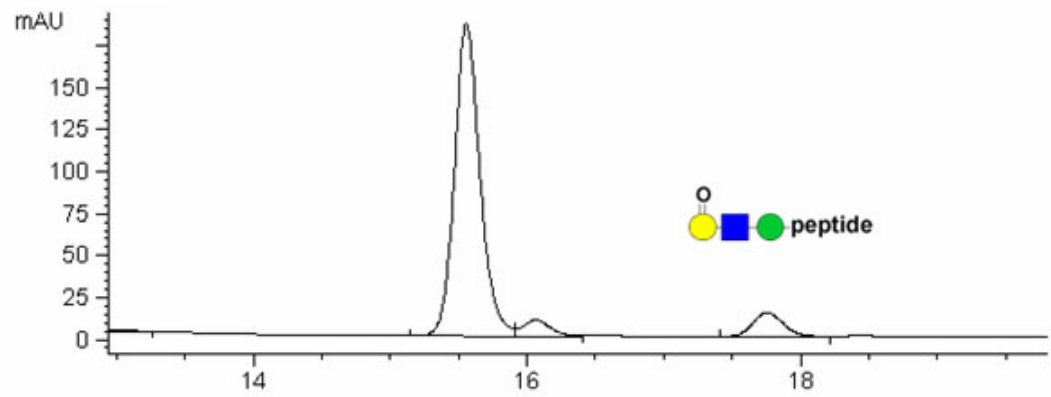
mAU
150
125
100
75
50
25
0
14
16
18
O
peptide

D

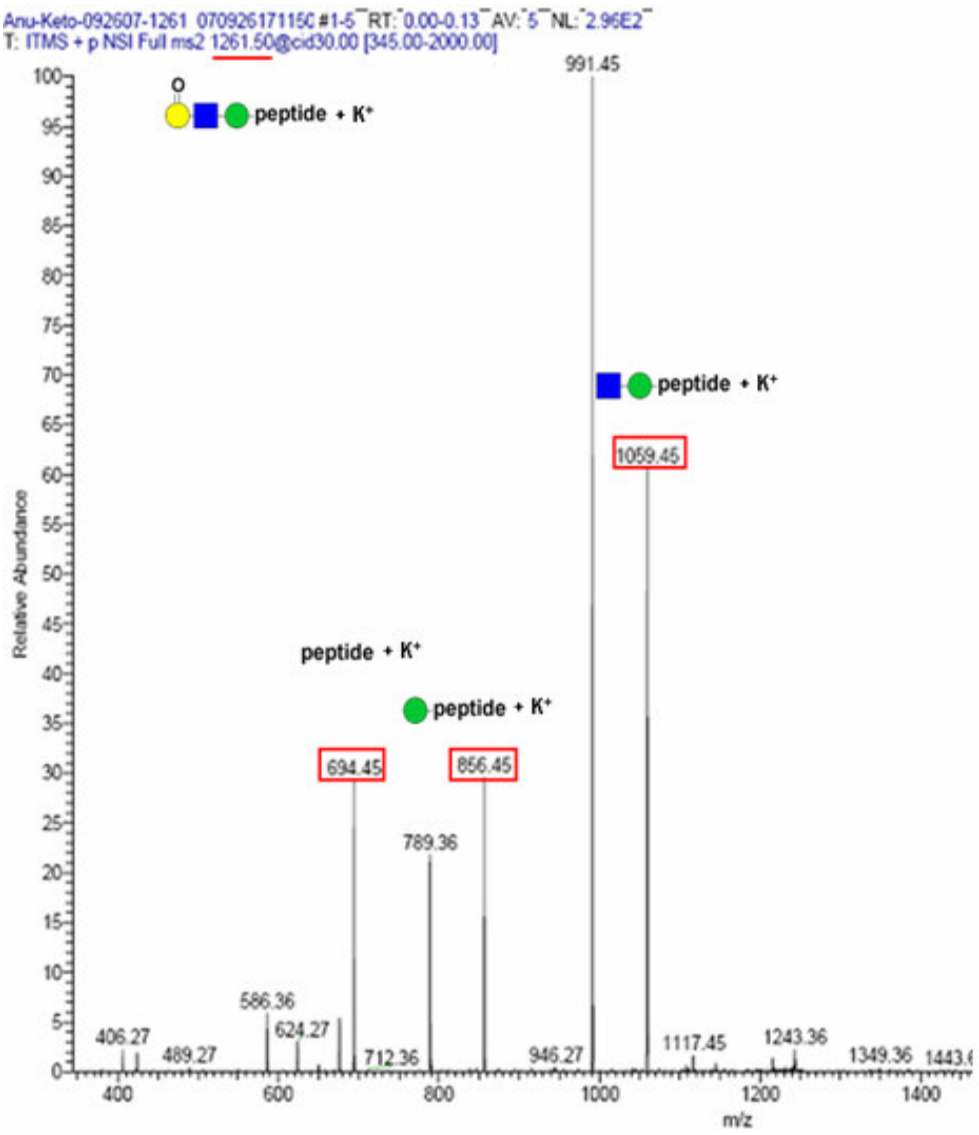
Anu-Keto-092607-1261 070926171150 #1-5 RT: 0.00-0.13 AV: 5 NL: 2.96E2
T: ITMS + p NSI Full ms2 1261.50@cid30.00 [345.00-2000.00]
peptide + K+
peptide + K+
peptide + K+
peptide + K+
991.45
1059.45
694.45
856.45
789.36
586.36
624.27
406.27
489.27
712.36
946.27
1117.45
1243.36
1349.36
Relative Abundance
m/z

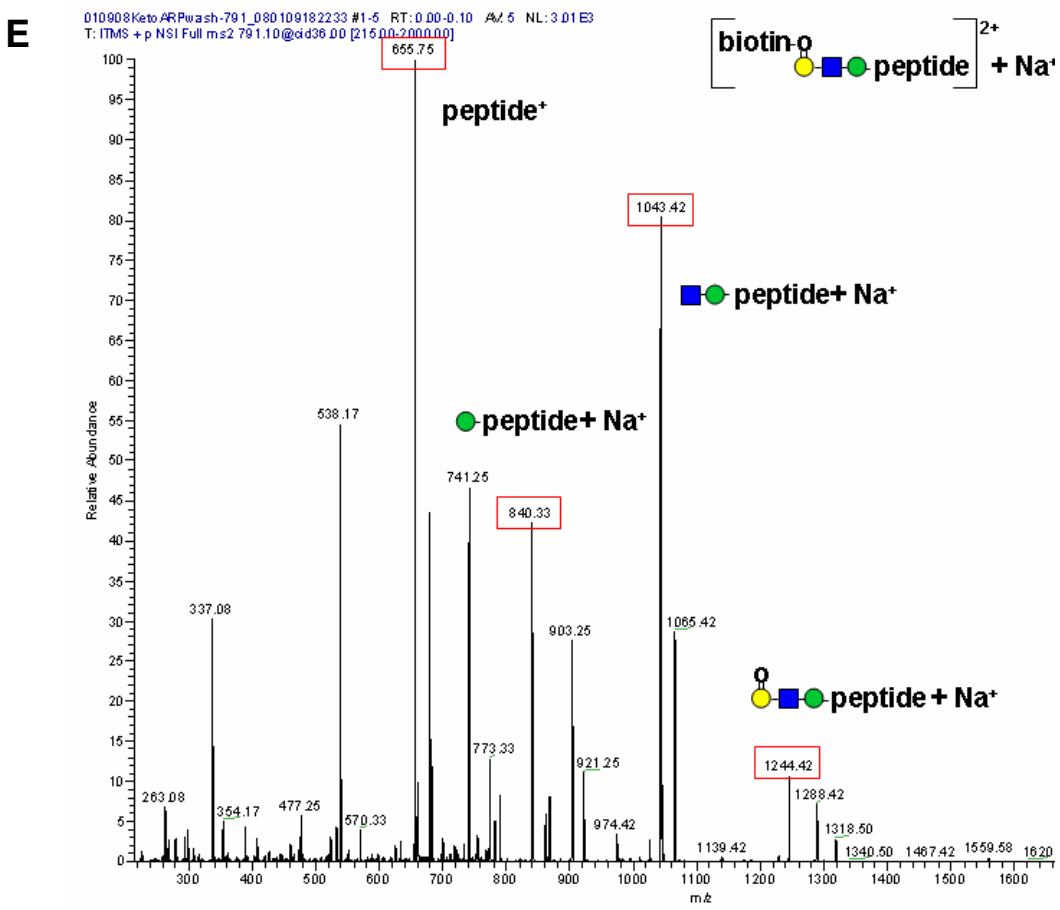

Figure 9. Evidence for the formation of the Gal(keto) product. HPLC traces monitoring the reaction at **(A)** time 0, **(B)** 24h after the addition of UDP-GlcNAc and POMGnT1, **(C)** 12h after the addition of Gal(keto) and Y289L GalT. **(D)** MS/MS fragmentation of 1261.50, the Gal(keto) product formed in **(C)**. Peptide sequence, Ac-VEPT(Man)AV-NH_2

can be successfully affinity purified and analyzed by direct infusion on the mass spectrometer (Figure 9E).

Neither azide, nor ketone modified sugars are biological molecules. However, enzymes recognize these molecules with a specificity that is similar to biological sugars. Moreover, the unique azide and ketone functionalities allow for a highly selective chemical reaction with reporter tags, thereby allowing for affinity purification and high-

throughput screening of O-mannose modified proteins. An advantage of the FLAG and biotin chemical probes is that they utilize novel chemical motifs to selectively react with their chemical reporter azide and ketone moieties.

OPTIMIZATION: As discussed in the previous section, lower product yield in the HPLC profiles for all reactions can be optimized by adding more enzyme in order to drive the reaction to completion. The low signal intensity in the mass spectrum for the GlcNAz product peak (Figure 7D) could be ameliorated by taking the reaction a step further and labeling the azide group with FLAG-phosphine. To avoid labeling terminal GlcNAcs on N-linked glycans and glycosaminoglycans in experiments using the brain protein powder and mutant Y289L galactosyltransferase, we propose using a cocktail of exoglycosidases and affinity chromatography as a control when we proceed with the actual sample (53). A pitfall in the current experimental method is that the Gal(keto)-biotin product elutes off the monomeric avidin resin into the wash buffer (data not shown). This can be corrected with a pre-clearing step of strong cation exchange to remove unreacted biotin probe that binds to the affinity matrix. Moreover, a polymer contaminant interferes with mass spectrometric analysis of the azido-FLAG product. We are in the process of rectifying these pitfalls, and also using the “click” chemistry kit before proceeding with the work described in Chapter 3.

CHAPTER 3

FUTURE DIRECTIONS

O-mannosylation plays an important role during mammalian neurogenesis and a severe phenotype has been associated with the loss-of-function of the glycosyltransferases that add and extend this moiety in CMDs. The protein α-DG is the most studied substrate in this context. Hypoglycosylated α-DG has been associated with oncogenesis and metastasis, which further underscores the significance of O-linked mannose in metazoans. However, the phenotype associated with a brain specific α-DG knockout does not correlate with the phenotypes associated with the loss-of-function of glycosyltransferases that function in the known O-mannose pathway, and a third of O-linked glycans in the brain are mannose-initiated structures. Given the implications of mannosylation in disease, this project developed a strategy to determine the identity and distribution of other POMT1/2 substrates. As discussed at the end of each section in chapter 2, certain reaction conditions require additional optimization. This chapter discusses potential experiments that can be conducted to further study O-mannosylation.

Identification of O-mannose modified proteins.

1. Chemoenzymatic labeling. Brain proteins from a mouse model of Muscle-Eye-Brain disease (work done in collaboration with Dr. Haiyu Hu, SUNY) and their wild-type littermates will be purified by organic extraction, delipidated and denatured as described in Chapter 2. The proteins will be subjected to enzymatic labeling, chemoselective

ligation, and affinity purification. As a negative control, UDP-GlcNAc and UDP-GalNAc will be used in the respective labeling experiments with POMGnT1 and Y289L GalT. Conditions will be optimized to account for labeling more O-mannosylated sites. Affinity purified eluates will be reduced, alkylated, trypsin digested, and passed again over the affinity column in order to enrich for mannosylated peptides.

2. Mass spectrometric analysis. All samples will be desalted over C18 reverse phase spin columns (Grace Vydac, Nest Group), and LC-MS/MS will be performed using C18 capillary columns (packed in-house) and standard laboratory procedures on a linear ion trap mass spectrometer (LTQ, LTQ-XL-ETD, or LTQ-Orbitrap).

3. Direct identification. An alternative strategy would attempt to purify and separate trypsin digested peptides via multidimensional protein identification technology (MudPIT). This would involve using strong cation exchange followed by reverse phase on an Agilent 1100 HPLC, before online LC-MS/MS on a linear ion trap (LTQ, ThermoFinnigan) as described earlier for affinity purified eluates. This approach could also utilize electron transfer dissociation (ETD) mass spectrometry and a high mass accuracy and high resolution LTQ-Orbitrap (ThermoFinnigan) in order to facilitate data acquisition.

4. Data analysis. Data will be analyzed via BioWorks using both forward and reverse mouse protein databases and a false-discovery rate of less than 1%. All mass spectrometric and data analysis techniques have been validated in this laboratory in previous and ongoing work (54), and are supported by the corresponding equipment.

5. Confirm protein identity via immunohistochemistry. To test and confirm the localization of potential candidate proteins that can be used for further study during the

remainder phases of the project, we plan to conduct immunohistochemical labeling using brain sections from the POMGnT1 knockout newborn and adult mouse (in collaboration with Dr. Haiyu Hu, SUNY) via commercially available antibodies against the candidate proteins. The control for these experiments will be brain slices from the wildtype mouse. This will allow us to compare morphological differences resulting from the loss of function of the O-mannosylated protein in question.

Completion of this segment will rely on the receipt of fixed, embedded, and sectioned brain tissue from the collaborator since it will be necessary to preserve tissue structure and properties of the antigen. An alternative would be to work with primary cells from the POMGnT1 knockout mouse brain in tissue culture. However, these have a limited lifespan, and also rely on another laboratory. In the event that neither is available, we propose to knockout the gene in an established neuronal cell line such as rat pheochromocytoma PC12 cells and correlate changes in phenotype with those observed upon deletion of α-DG. This assumes that glycosylation plays a similar role in this protein's function as it does in α-DG.

Mapping the sites of O-mannosylation on a protein of interest.

Following identification of O-mannose modified proteins in the total mouse proteome, we will select a protein of biological interest that has been implicated in disease processes. It will be necessary to site-map O-mannosylated sites before proceeding to elucidate O-mannose function via site-directed mutagenesis. However, O-linked mannosylation is one of the most complicated post-translational modifications for site-mapping analysis. This is because there is no consensus sequence for O-mannosylation (data not shown), O-glycosylated sites are often adjacent to each other

and these can also harbor non-glycosylated serines and threonines (52), and the glycosidic bond is labile under collision induced dissociation (CID) mass spectrometry. In addition to this, fragmentation corresponding to the loss of the glycan leaves the site of attachment unmodified (55). To sidestep these limitations, we propose to analyze data from a combination of various site-mapping strategies that have been validated in this laboratory, and are supported by the corresponding mass spectrometric equipment.

1. Protein purification. Site-mapping demands the use of purified protein. We propose to employ several approaches towards protein purification. Brain proteins from a wild-type mouse (Pel-Freeze) will be purified by organic extraction, delipidated and denatured as described in Chapter 2. These will be separated via size exclusion and immunoaffinity chromatography. Lectin affinity chromatography is also a useful step that will ensure separation of glycoproteins from the sample. However, N-linked glycans and glycosaminoglycans can also bind to the column, and an intermediate step would involve using glycosidases to cleave off inapplicable structures. Size exclusion chromatography offers low resolution separation, and consequently can be coupled with immunopurification using commercially available antibodies that recognize the protein covalently linked to protein-A/G agarose beads. This last approach will isolate all glycoforms of the protein. The eluates from chromatography columns can be run on either a 1D or 2D SDS-PAGE gel, or a PF-2D instrument so as to confirm purification of the protein and to resolve co-purifying species (53). A practical alternative to these approaches would be to procure the protein through collaboration with another laboratory.

2. Protein site-mapping. Purified protein will be subjected to reduction, carboxyamidomethylation, and enzymatic digestion using either trypsin, lysC, gluC, or a combination of these. Site-mapping of the peptides will be conducted using the following techniques.

a. Pseudo-neutral loss MS^n. Trypsin digested peptides will be analyzed directly by LC-MS^3 on a linear ion-trap (LTQ, Thermo Finnigan) using automated MS^3 sequencing upon detection of the neutral loss of a molecular mass corresponding to an expected glycan in MS^2. The POMGnT1 mouse brain knockout glycome has already been characterized (Figure 3), and previous work conducted in the laboratory on α-DG has identified 40 unique glycopeptides and 10 O-mannosylation sites (unpublished data).

b. Beta-elimination followed by Michael addition with dithiolthreitol (BEMAD).

Alkaline-induced β-elimination of O-glycans generates an α,β-unsaturated carbonyl dehydroamino acid which can be tagged by the Michael addition of dithiolthreitol (DTT) and analyzed via LC-MS/MS on an LTQ instrument. This technique has been validated for site-mapping both O-GlcNAc and O-Mannose modified proteins. Compared to native glycosylation, DTT is a stable under CID, and DTT modified peptides can be purified via thiol chromatography. Isotope labeled DTT can also be used for quantification (56,57).

c. Electron transfer dissociation (ETD) of multiply charged peptides.

Compared to CID which fragments ions in the gas phase based on collision with a neutral gas, ETD induces fragmentation by transferring electrons to ions. As a result, ETD cleaves the peptide backbone and preserves glycosidic linkages. However, this technique works mainly with higher charge states ($z>2$) and requires sample

preparation using either gluC, or lysC instead of trypsin (58). This technique has been validated using both O-Man and O-GlcNAc peptides.

The LTQ-XL-ETD mass spectrometer (ThermoFinnigan) in the laboratory allows for both CID and ETD based fragmentation. Consequently, a full MS scan of the peptides during LC-MS/MS on a C18 reverse phase column can be followed by both pseudo-neutral loss MS^n and ETD fragmentation of the most abundant peaks in the chromatogram. These techniques will aid in mapping O-mannose to specific sites. Site-mapping techniques such as the pseudo-neutral loss method are restricted by the fact that mannose has the same mass-to-charge value as glucose. As mentioned earlier, there is no consensus sequence for O-mannosylation. However, O-linked glucose has a consensus sequence. Moreover, in the event that a site cannot be mapped, samples can be subjected to exo- and endo-glycosidase digestions to remove specific structures and the experiments can be conducted again.

Establishing a structure-function relationship for O-mannose initiated glycans on the site-mapped protein.

1. Binding studies. Our laboratory has used surface plasmon resonance (BiaCore T100 and T3000) for establishing a direct link between the effects of glycosylation on α-DG's binding kinetics with laminin-1 (work done by Dr. Gerardo Gutiérrez-Sánchez, data not shown). For this experiment, AEBSF treated laminin-1 was biotinylated with sulfo-NHS biotin and immobilized on a streptavidin chip at 285 resonance units. α-DG was treated overnight with various glycosidases and 200nM of this sample was injected over the chip to monitor laminin binding. A similar strategy will be adopted for the O-mannosylated protein. The purified protein can be treated with a host of glycosidases,

and its binding kinetics monitored with an interacting partner immobilized on a chip. The corollary to this experiment will involve immobilizing the protein on the chip and injecting the binding partner over the surface of the chip. The data derived from these experiments will isolate the key functional sites of O-mannosylation and the structures that modulate protein binding. A ligand overlay and solid-phase binding assay can be performed as a preliminary experiment in order to confirm and quantify ligand binding activity.

2. Tissue culture. Another approach to study O-mannose in protein function would involve creating site-directed mutations on the protein, and overexpressing these in an immortalized neuronal cell line. Primary cultured neurons of the POMGnT1 knockout mouse brain would be useful in this study. Overexpression of the native protein should rescue the neurite outgrowth phenotype associated with the loss-of-function of POMGnT1 (19). However, this experiment relies on collaboration with another lab (Dr. Hyaiyu Hu, SUNY).

An immortalized cell line would be selected based on previous work conducted on the protein of interest. The main factors towards selecting a cell line include its gene expression pattern, developmental history, function, dendritic morphology, and axonal projections. Either rat pheochromocytoma PC12 cell line, or the neuroblastoma cell line SHSY5Y (ATCC) would be ideal since they have been used in previous studies for studying cell-matrix interactions (51,59). The culture conditions will be used as per those specified by ATCC. A construct bearing a site mutation in the protein will be transfected via Lipofectoamine 2000 (Invitrogen), and changes in cell phenotype will be monitored. Cell adhesion, scratch wound, and neurite outgrowth assays will be

performed as previously described (51,59). Immunoprecipitation, ligand overlay assay and a solid-phase binding assay will be employed in combination with deglycosylation experiments in order to correlate phenotypic changes with protein glycosylation.

Genetics in *Caenorhabditis elegans*

Caenorhabditis elegans is often used in neuroscience studies that involve genetic manipulation. It has a short generation time, transparent body, simple organs, and conserved molecular mechanisms in comparison to vertebrates. It has 302 neurons each of which has a known lineage, connectivity, and function, and approximately 100 genes that are homologous to those implicated in human diseases (60). A POMGnT1 knockout of *C. elegans* is an embryonic lethal (61,62), which validates *C. elegans* as an organism with functionally relevant O-mannosylation that mimics mammalian systems.

However, there are a number of drawbacks to experiments that would use this organism. Studies have shown that the structural organization of the basement membrane with muscle cells and at neuromuscular junctions is different in nematodes (63). Moreover, it will be necessary to confirm that the *C. elegans* protein is similar to its vertebrate orthologues and to select a gene based on genomic sequence analysis. The *C. elegans* O-glycome has unusual structures (64), which will have to be characterized and confirmed. And while the functional role of the *C. elegans* N-glycome has been studied (65), no research has been conducted on the O-glycans. It will thus be necessary to conduct preliminary studies to correlate O-glycan function with mammalian glycan structures, since it is not known whether O-mannose plays a similar role in the nematode as it does in mammals. Additionally, while our laboratory has the technical expertise to maintain the nematode, we have not developed efficient transfection

methods for generating the transgenics that will be a necessary first step towards loss-of-function and gain-of-function studies.

C. elegans experiments would be a useful future step towards *in vivo* structure-function studies of O-mannose. *Drosophila melanogaster* is another popular model organism, and it has been shown that the loss of function of dPOMT1 and dPOMT2 mediated glycosylation is associated with neuron migration defects (21,22). Both *C. elegans* (66,67) and *D. melanogaster* (68,69) have been used in studies of the dystrophin-glycoprotein complex. However, there are no known extended O-mannose structures in *D. melanogaster* (in correspondence, Dr. K. Aoki), which eliminates it as a potential organism for *in vivo* studies targeted towards studying mammalian O-mannosylation.

As described in this chapter, state-of-the-art mass spectrometric equipment and novel chemoenzymatic labeling procedures will help generate a qualitative report of the entire range of neuronal O-mannosylated proteins. Following this identification, O-mannose will be site-mapped on a specific protein of biological importance and the exact nature of mannose's structure-function relationship will be determined. Glycosylation site-mapping techniques have been optimized in previous work done by the laboratory using α-DG and are corroborated by the corresponding equipment. Future efforts will concentrate on probing the function of the protein using binding assays and model systems such as neuronal cell lines and the nematode *C. elegans*. A combination these experiments will help better understand O-mannose function in tissue, and the specific role that it plays in human diseases.

REFERENCES

1. Sentandreu, R., and Northcote, D. . (1969) *Carbohydrate Research* **10**, 584-585
2. Finne, J., Krusius, T., Margolis, R. K., and Margolis, R. U. . (1979) *Journal of Biological Chemistry* **254**, 10295-10300
3. Krusius, T., Reinhold, V. N., Margolis, R. K., and Margolis, R. U. . (1987) *Biochemical Journal* **245**, 229-234
4. Chiba, A., Matsumura, K., Yamada, H., Inazu, T., Shimizu, T., et. al. (1997) *Journal of Biological Chemistry* **272**, 2156-2162
5. Yuen, C.-T., Chai, W., Loveless, R. W., Lawson, A. M., Margolis, R. U., et. al. (1997) *Journal of Biological Chemistry* **272**, 8924-8931
6. Willer, T., Valero, M. C., Tanner, W., Cruces, J., and Strahl, S. (2003) *Current Opinion in Structural Biology* **13**, 621-630
7. Endo, T., and Toda, T. . (2003) *Biological and Pharmaceutical Bulletin* **26**, 1641–1647
8. Martin, P. T. (2003) *Glycobiology* **13**, 55R-66R
9. Chai, W., Yuen, C-T., Kogelberg, H., Carruthers, R. A., Margolis, R. U., et. al. . (1999) *European Journal of Biochemistry* **263**, 879-888
10. Strahl-Bolsinger, S., Gentzsch, M., and Tanner, W. (1999) *Biochimica et Biophysica Acta* **1426**, 297-307
11. Barresi, R., and Campbell, K. (2006) *Journal of Cell Science* **119**, 199-207
12. Krusius, T., Finne, J., Margolis, R. K., and Margolis, R. U. . (1986) *Journal of Biological Chemistry* **261**, 8237-8242

13. Endo, T. (2004) *Glycoconjugate Journal* **21**, 3-7

14. Yoshida, A., Kobayashi, K., Manya, H., Taniguchi, K., Kano, H., et. al. (2001) *Developmental Cell* **1**, 717-724

15. Prescher, J. A., and Bertozzi, C. R. (2005) *Nature Chemical Biology* **1**, 13-21

16. Beltrán-Valero de Bernabé, D., Currier, S., Steinbrecher, A., Celli, J., van Beusekom, E., et. al. (2002) *The American Journal of Human Genetics* **71**, 1033-1043

17. van Reeuwijk, J., Janssen, M., van den Elzen, C., Beltran-Valero de Bernabé, D., Sabatelli, P., et. al. (2005) *Journal of Medical Genetics* **42**, 907-912

18. Liu, J., Ball, S. L., Yang, Y., Mei, P., Zhang, L. et. al. . (2006) *Mechanisms of Development* **123**, 228-240

19. Hu, H., Yang, Y., Eade, A., Xiong, Y., and Qi, Y. (2007) *Journal of Comparative Neurology* **501**, 168-183

20. Yang, Y., Zhang, P., Xiong, Y., Li, X., Qi, Y., et. al. . (2007) *Journal of Comparative Neurology* **505**, 459-477

21. Martin-Blanco, E., and Garcia-Bellido, A. . (1996) *Proceedings of the National Academy of Sciences* **93**, 6048-6052

22. Ichimiya, T., Manya, T. H., Ohmae, Y., Yoshida, H., Takahashi, K., et. al. . (2004) *Journal of Biological Chemistry* **279**, 42638-42647

23. Michele, D. E., and Campbell, K. P. . (2003) *Journal of Biological Chemistry* **278**, 15457-15460

24. Zaccaria, M. L., Di Tommaso, F., Brancaccio, A., Paggi, P., and Petrucci, T. C. . (2001) *Neuroscience* **104**, 311-324

25. Moore, S. A., Saito, F., Chen, J., Michele, D. E., Henry, M. D., et. al. . (2002) *Nature* **418**, 422-425

26. Martin, P. T., and Freeze, H. H. (2003) *Glycobiology* **13**, 67R-75R

27. Bogdanik, L., Framery, B., Frölich, A., Franco, B., Mornet, D., et. al. . (2008) *PLoS ONE* **3**, e2084

28. Peng, H. B., Ali, A. A., Daggett, D. F., Rauvala, H., Hassell, J. R., et. al. . (1998) *Cell Adhesion and Communication* **5**, 475-489

29. Bülow, H. E., and Hobert, O. (2006) *Annual Reviews Cell and Developmental Biology* **22**, 375-407

30. Ramakrishnan, B., and Qasba, P. K. (2002) *Journal of Biological Chemistry* **277**, 20833-20840

31. Khidekel, N., Arndt, S., Lamarre-Vincent, N., Lippert, A., Poulin-Kerstien, K. G., et. al. . (2003) *Journal of the American Chemical Society* **125**, 16162-16163

32. Saxon, E., and Bertozzi, C. R. (2000) *Science* **287**, 2007-2010

33. Agard, N. J., Prescher, J. A., and Bertozzi, C. R. (2004) *Journal of the American Chemical Society* **126**, 15046 -15047

34. Vocadlo, D. J., Hang, H. C., Kim, E-J., Hanover, J. A., and Bertozzi, C. . (2003) *Proceedings of the National Academy of Sciences* **100**, 9116-9121

35. Hang, H. C., Yu, C., Kato, D. L., and Bertozzi, C. R. (2003) *Proceedings of the National Academy of Sciences* **25**, 14846-14851

36. Kiick, K. L., Saxon, E., Tirrell, D. A., and Bertozzi, C. R. (2002) *Proceedings of the National Academy of Sciences* **99**, 19-24

37. Kohn, M., Wacker, R., Peters, C., Schroder, H., Soulere, L., et. al. (2003) *Angewandte Chemie (International edition in English)* **42**, 5830-5834

38. Luchansky, S. J., Argade, S., Hayes, B. K., and Bertozzi, C. R. (2004) *Biochemistry* **43**, 12358-12366

39. Huisgen, R. (1963) *Angewandte Chemie (International edition in English)* **2**, 565-598

40. Tornoe, C. W., Christensen, C., and Meldal, M. (2002) *Journal of Organic Chemistry* **67**, 3057-3064

41. Rostovtsev, V. V., Green, L. G., Fokin, V. V., and Sharpless, K. B. (2002) *Angewandte Chemie* **114**, 2708-2711

42. Speers, A. E., and Cravatt, B. F. (2004) *Chembiochem* **5**, 41-47

43. Seo, T. S., Bai, X., Ruparel, H., Li, Z., Turro, N. J. et. al. . (2004) *Proceedings of the National Academy of Sciences* **101**, 5488-5493

44. Wang, Q., Chan, T. R., Hilgraf, R., Fokin, V. V., Sharpless, K. B., et. al. . (2003) *Journal of the American Chemical Society* **125**, 3192-3193

45. Khidekel, N., Ficarro, S. B., Peters, E. C., and Hsieh-Wilson, L. (2004) *Proceedings of the National Academy of Sciences* **101**, 13132-13137

46. Rideout, D. (1994) *Cancer Investigation* **12**, 189-202

47. Qasba, P., Ramakrishnan, B., and Boeggeman, E. (2006) *The AAPS Journal* **8**, E190-E195

48. Lennarz, W. J., and Hart, G. W. . (1994) *Methods in Enzymology* **230**, 57-66

49. Aoki, K., Perlman, M., Lim, J-M., Cantu, R., Wells, L., et. al. . (2007) *Journal of Biological Chemistry* **282**, 9127-9142

50. Zhang, W., Betel, D., and Schachter, H. . (2002) *Biochemical Journal* **361**, 153–162

51. Abbott, K. L., Troupe, K., Lee, I., and Pierce, M. . (2006) *Experimental Cell Research* **312**, 2837-2850

52. Whelan, S. A., and Hart, G. W. . (2006) *Methods in Enzymology* **415**, 113-133

53. Ervasti, J. M., S. D. Kahl, and Campbell, K. P. . (1991) *Journal of Biological Chemistry* **266**, 9161-9165

54. Lim, J.-M., Sherling, D., Teo, C. F., Hausman, D. B., Lin, D., et. al. (2007) *Journal of Proteome Research* **7**, 1251-1263

55. Greis, K. D., and Hart, G. W. (1998) *Methods in Molecular Biology* **76**, 19-33

56. Wells, L., Vosseller, K., Cole, R. N., Cronshaw, J. M., Matunis, M. J., et. al. . (2002) *Molecular and Cellular Proteomics* **1**, 791-804

57. Vosseller, K., Hansen, K. C., Chalkley, R. J., Trinidad, J. C., Wells, L., et. al. . (2005) *Proteomics* **5**, 388-398

58. Mikesh, L. M., Ueberheide, B., Chi, A., Coon, J. J., Syka, J. E. P., et. al. . (2006) *Biochimica et Biophysica Acta* **1764**, 1811-1822

59. Lee, I., Guo, H-B, Kamar, M., Abbott, K., Troupe, K., et. al. . (2006) *Journal of Neurochemistry* **97**, 947-956

60. Culetto, E., and Sattelle, D.B. . (2000) *Human Molecular Genetics* **9**, 869-877

61. Kamath, R. S., Fraser, A. G., Dong, Y., Poulin, G., Durbin, R., et. al. . (2003) *Nature* **421**, 231-237

62. Sönnichsen, B., Koski, L. B., Walsh, A., Marschall, P., Neumann, B., et. al. . (2005) *Nature* **434**, 462-469

63. Hrus, A., Gordon, L., Hutter, H., Schenk, S., Ferralli, J., et. al. . (2007) *PLoS ONE* **2**, e731

64. Haslam, S. M., Gems, D., Morris, H. R., and Dell, A. . (2002) *Biochemical Society Symposia* **69**, 117-134

65. Schachter, H., Chen, S., Zhang, W., Spence, A. M., Zhu, S., et. al. . (2002) *Biochemical Society Symposia* **69**, 1-21

66. Grisoni, K., Martin, E., Gieseler, K., Mariol, M-C., and Se´galat, L. . (2002) *Gene* **294**, 77-86

67. Johnson, R. P., Kang, S. H., and Kramer, J. M. . (2006) *Development* **133**, 1911-1921

68. Greener, M. J., and Roberts, R. G. . (2000) *FEBS Letters* **482**, 13-18

69. Dekkers, L. C., van der Plas, M. C., van Loenen, P. B., den Dunnen, J. T., van Ommen, G. J., et. al. . (2004) *Gene Expression Patterns* **4**, 153-159